arXiv:2504.09185v1 [cs.LG] 12 Apr 2025

Highlights

Repetitive Contrastive Learning Enhances Mamba's Selectivity in Time Series Prediction

Wenbo Yan, Hanzhong Cao, Ying Tan

- A token-level training paradigm named Repeating Sequence Augmentation is proposed. Through the repetition of timesteps and the introduction of noise, combined with intra-sequence and inter-sequence contrastive learning, the parameters of the Mamba block are enabled to identify key timesteps and ignore noise.
- RCL is integrated into the training process of various Mamba-based models, with the parameters obtained from RCL being utilized as the initialization for the backbone model's parameters, thereby further enhancing the temporal prediction capabilities of the backbone model.
- It is demonstrated that RCL can significantly improve the performance of backbone models, and its broad effectiveness for Mamba-based models is proven without incurring additional memory overhead through experiments.
- The impact of different parameter replacement methods and freezing techniques is experimentally analyzed.
- Two metrics are proposed to measure the selective capabilities of Mamba. The effectiveness of RCL is demonstrated from theoretical, qualitative, and quantitative perspectives.

Repetitive Contrastive Learning Enhances Mamba's Selectivity in Time Series Prediction

Wenbo Yan[1,a,b], Hanzhong Cao[1,a], Ying Tan[a,c,d,e]

[a]*School of Intelligence Science and Technology, Peking University, Beijing,*
[b]*Computational Intelligence Laboratory,*
[c]*Institute for Artificial Intelligence,*
[d]*National Key Laboratory of General Artificial Intelligence,*
[e]*Key Laboratory of Machine Perceptron (MOE),*

Abstract

Long sequence prediction is a key challenge in time series forecasting. While Mamba-based models have shown strong performance due to their sequence selection capabilities, they still struggle with insufficient focus on critical time steps and incomplete noise suppression, caused by limited selective abilities. To address this, we introduce Repetitive Contrastive Learning (RCL), a token-level contrastive pretraining framework aimed at enhancing Mamba's selective capabilities. RCL pretrains a single Mamba block to strengthen its selective abilities and then transfers these pretrained parameters to initialize Mamba blocks in various backbone models, improving their temporal prediction performance. RCL uses sequence augmentation with Gaussian noise and applies inter-sequence and intra-sequence contrastive learning to help the Mamba module prioritize information-rich time steps while ignoring noisy ones. Extensive experiments show that RCL consistently boosts the performance of backbone models, surpassing existing methods and achieving state-of-the-art results. Additionally, we propose two metrics to quantify Mamba's selective capabilities, providing theoretical, qualitative, and quantitative evidence for the improvements brought by RCL.

Keywords:
Time Series Forecasting, Long Sequence Prediction, Mamba, Repetitive Contrastive Learning, Selectivity Measurement

1. Introduction

Time series forecasting (TSF) has become indispensable across a range of critical domains, including financial markets (Li et al., 2023), traffic management (Cheng et al., 2023), electricity consumption prediction (Sun and Zhang, 2023), scientific computing (Cruz-Camacho et al., 2024), and weather forecasting (Zhang et al., 2022a). TSF leverages sequential data—often irregular, incomplete, or noisy—to predict future trends based on past observations. Yet, fully reliable forecasting remains elusive, largely due to the opaque generative processes behind time series data. These complexities are exacerbated by uneven sampling, missing or redundant entries, and unpredictable disturbances.(Zhu et al., 2023)(Ramponi et al., 2019) In such a setting, designing models that not only process temporal sequences but also learn to focus on the most informative and structurally meaningful parts of the data becomes vital—hinting at the importance of aligning training objectives with the intrinsic dynamics of time series itself.(Nam et al., 2024)

Deep learning has advanced significantly in the time series domain, with much of the attention placed on architectural innovations, particularly in transformer-based models (Wen et al., 2023). Despite their success in NLP, transformers often struggle with the sequential and noisy nature of time series, underperforming compared to traditional architectures like CNNs and MLPs (Zeng et al., 2022). These conventional models, while limited in modeling long-range dependencies, excel at handling noise and capturing local patterns, contributing to their relative success in this domain. The emergence of the Mamba model (Gu and Dao, 2024) has further shifted attention toward architectures tailored for temporal data. Leveraging a selective state-space mechanism (Huang et al., 2024; Li et al., 2024), Mamba addresses the quadratic complexity of transformers while preserving their long-range propagation ability. Its success in recent time series forecasting models, such as TimeMachine (Ahamed and Cheng, 2024) and Bi-Mamba (Liang et al.,

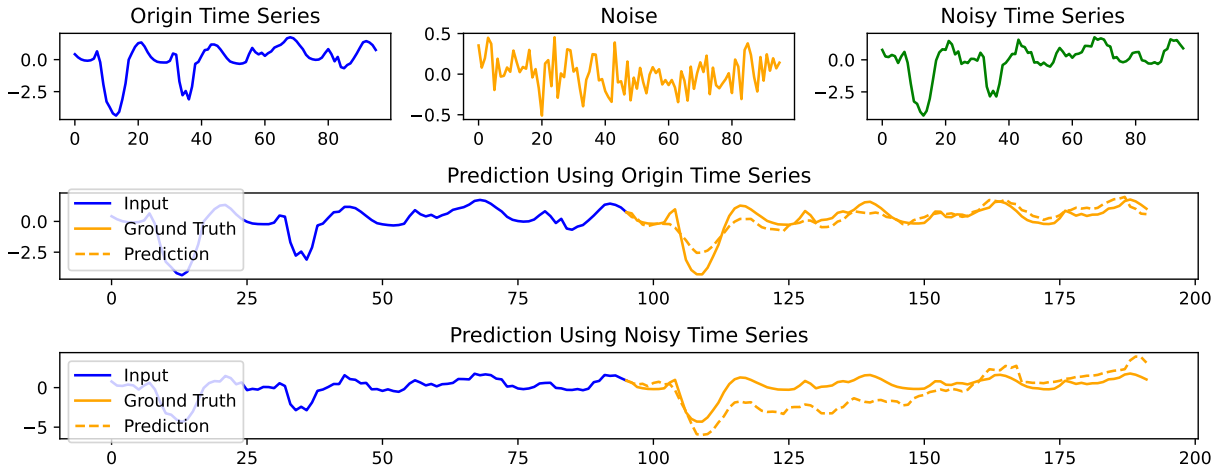

Figure 1: Impact of Noise Sensitivity on Prediction Results

2024), underscores the potential of this approach. However, these efforts often overlook a core challenge in time series: enabling models to identify and prioritize key timesteps amidst noise, a capability essential for robust and interpretable forecasting.

Although Mamba introduces a degree of selectivity by generating its state transition and input matrices dynamically based on time steps, this very mechanism also makes it more sensitive to temporal fluctuations and noise. As illustrated in Figure 1, Mamba exhibits two key limitations when predicting time series. On one hand, it fails to effectively focus on salient time steps, resulting in an inability to fit extreme cases such as sharp declines or rapid rises. On the other hand, Mamba is highly sensitive to noise, where even minor noise disturbances can lead to significant deviations in prediction results. This is attributed to insufficient selective capabilities of Mamba, causing noise to accumulate progressively during sequence modeling, ultimately amplifying small noise into large deviations. These limitations arise from its origins in natural language processing (NLP), where each token typically carries rich semantic meaning. In contrast, time series data often exhibit irregular sampling, low signal-to-noise ratios, and a lack of contextual semantics, making them fundamentally different from NLP data. Prior studies have also shown that directly applying NLP-inspired architectures to time series tasks yields suboptimal results (Zhang et al., 2024).

To address these shortcomings, we propose a token-level pre-training method specifically designed to enhance the initialization of the Mamba block, termed Repetitive Contrastive Learning (RCL). This approach aims to endow the Mamba architecture with stronger selective capabilities—enabling it to better attend to salient time steps while ignoring irrelevant or noisy ones. Importantly, the resulting initialization parameters are architecture-agnostic and can be flexibly applied to any model employing the Mamba block, thereby strengthening its capacity to model complex temporal dependencies.

Specifically, RCL is a novel pre-training framework comprising two key steps: Repeating Sequence Augmentation and Repetitive Contrastive Learning, meticulously designed to address the dual challenges of denoising and memorization. In the Repeating Sequence Augmentation step, each token in the sequence is duplicated and perturbed with Gaussian noise to simulate the irregular and redundant patterns commonly observed in real-world time series. Subsequently, during the Repetitive Contrastive Learning phase, we enhance the model's ability to ignore noisy timesteps through **intra-sequence contrast**, thereby suppressing spurious fluctuations. Simultaneously, **inter-sequence contrast** ensures the consistency of temporal features across sequences of varying lengths, preventing the loss of temporal variation extraction capabilities caused by repetitive augmentation and noise introduction. These two contrastive mechanisms collectively imbue Mamba with sharper selective capabilities and higher temporal fidelity, ultimately enabling more robust performance across diverse time series forecasting tasks.

We integrate this training paradigm into the training process of Mamba-based models by employing RCL to train a single Mamba block, obtaining parameters with enhanced selectivity. These parameters are then used as the initialization parameters for all Mamba blocks within the model, thereby boosting the overall predictive capability.

Experimental evaluations on multiple Mamba-based models demonstrate that our approach significantly enhances the predictive performance of the backbone models, achieving state-of-the-art (SOTA) results without incurring additional memory overhead. Furthermore, we explore module replacement and parameter freezing strategies to maximize transferability and training stability.

In summary, our main contributions are as follows:

- We propose a token-level training paradigm called Repeating Sequence Augmentation. By repeating timesteps and introducing noise, combined with intra-sequence and inter-sequence contrastive learning, the parameters of the Mamba block acquire the ability to identify key timesteps and ignore noise.
- We integrate RCL into the training process of various Mamba-based models, utilizing the parameters obtained from RCL as the initialization for the backbone model's parameters, further enhancing the temporal prediction capabilities of the backbone model.
- Experiments demonstrate that RCL can significantly improve the performance of backbone models, and its broad effectiveness for Mamba-based models is verified without incurring additional memory overhead. And the impact of different parameter replacement methods and freezing techniques is analyzed through experiments.

2. Preliminary

2.1. Multivariate Time Series Forecasting

Multivariate time series forecasting involves predicting future values of multiple interrelated time-dependent variables based on their historical data. Unlike univariate time series forecasting, which focuses on a single variable, multivariate forecasting accounts for interactions and correlations between multiple variables to improve prediction accuracy and insightfulness.

A multivariate time series forecasting problem can be formally represented with an input time series denoted as $\mathbf{X} \in \mathbb{R}^{T_{\text{in}} \times F}$, where T_{in} is the input sequence length (number of time steps) and F represents the number of features or variables at each time step. The prediction target is represented as $\mathbf{Y} \in \mathbb{R}^{T_{\text{out}} \times F}$, where T_{out} denotes the output sequence length for which forecasts are made.

2.2. Mamba Block

The Mamba block, (Gu and Dao, 2024), consists of two parts : selection and State Space Model (SSM), as shown in Fig. 2. Firstly, the input $\mathbf{X}$ undergoes a one-dimensional convolution (Conv1d) to extract local features, followed by Linear Projection that maps it to matrices $\mathbf{B}$, $\mathbf{C}$, and Δ.

$$\begin{aligned} \mathbf{X}_c &= \sigma(\text{Conv1d}(\mathbf{X})) \\ \mathbf{B} &= \text{fc}(\mathbf{X}_c), \quad \mathbf{C} = \text{fc}(\mathbf{X}_c) \\ \Delta &= \text{softplus}(\text{fc}(\mathbf{X}_c) + \mathbf{A}) \end{aligned} \tag{1}$$

where σ is SiLU activation function and softplus means the Softplus activation functions, and $\mathbf{A}$ is an optimizable matrix. Then, matrices $\mathbf{A}$ and $\mathbf{B}$ are discretized into $\overline{\mathbf{A}}$, $\overline{\mathbf{B}}$,

$$\begin{aligned} \overline{\mathbf{A}} &= \exp(\Delta \mathbf{A}) \\ \overline{\mathbf{B}} &= (\exp(\Delta \mathbf{A}) - \mathbf{I})(\Delta \mathbf{A})^{-1}(\Delta \mathbf{B}) \end{aligned} \tag{2}$$

Finally, Mamba inputs $\overline{\mathbf{A}}$, $\overline{\mathbf{B}}$, $\mathbf{C}$, Δ, and $\mathbf{X}$ into the SSM, and uses residual connections.

$$\mathbf{H} = \text{SSM}(\overline{\mathbf{A}}, \overline{\mathbf{B}}, \mathbf{X}) \cdot \sigma(\text{fc}(\mathbf{X})) \tag{3}$$

where fc is fully connected layers, and σ is SiLU activation function. The computational process of the State Space Model (SSM) can be succinctly represented as follows:

$$\begin{aligned} \mathbf{h}_t &= \overline{\mathbf{A}}\mathbf{h}_{t-1} + \overline{\mathbf{B}}\mathbf{x}_t \\ \mathbf{o}_t &= \mathbf{C}\mathbf{h}_t \end{aligned} \tag{4}$$

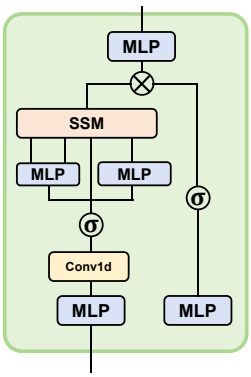

Figure 2: The structure of the mamba block.

2.3. Definition of Mamba's Selectivity

The selectivity of Mamba primarily stems from its unique Selective State Space Model (SSM). The computational process of the SSM is shown in Eq.4. Unlike traditional SSMs (Gu et al., 2022), the state transition matrix $\overline{\mathbf{A}}$ and the input matrix $\overline{\mathbf{B}}$ are derived from the current timestep. As a result, the state transition matrix and input matrix generated based on the timestep can selectively decide whether to retain more historical state information or incorporate more information from the current timestep (Gu and Dao, 2024).

We uniformly define the incorporation of more current timestep information as **memory** and the retention of more historical state information as **ignoring**. We define Mamba's Selectivity as the ability to prominently choose between memorizing and ignoring new timestep information under the current historical state, where it more prominently memorizes important timesteps while more prominently ignores noisy timesteps. As discussed in Section 2.2, Mamba's Selectivity arises from three key components: the matrices $\mathbf{A}$, $\mathbf{B}$, and the discretization parameter Δ.

2.4. Definition of a Selectivity Measurement

Since Mamba, unlike Transformer, does not provide explicit attention scores to intuitively measure selectivity, understanding how it retains or discards information requires alternative strategies. While Mamba is based on a Selective State Space Model (SSM) rather than a gated recurrent mechanism, it shares with RNNs and LSTMs the key characteristic of processing sequences in a token-by-token manner, rather than consuming entire sequences simultaneously as Transformers do. This temporal nature of computation motivates us to draw inspiration from prior works analyzing memory and information retention in RNNs, where token-level dynamics — such as the evolution of hidden states across time — have been used to study memory behaviors (Zhang et al., 2020; Haviv et al., 2019).

Building on this perspective, we propose two quantitative metrics to assess the selectivity of Mamba. First, based on Eq. 4, we compute the correlation between the current hidden state h_t, the previous hidden state h_{t-1}, and the current input x_t, normalizing the results to sum to 1. We define the correlation with x_t as the **memory score** s_t at the current time step. Following the definitions of memory and ignoring from Section 2.3, we categorize time steps with $s_t > 0.7$ as **Significant Memory (SM)**, those with $s_t < 0.3$ as **Significant Ignoring (SI)**, and the remainder as **Normal (NR)**. This approach is in line with previous efforts to quantify memory at each time step in sequential models by examining how hidden representations evolve over time (Ming et al., 2017). Based on these memory scores, we define two Selectivity Measurements: **Focus Ratio** and **Memory Entropy**.

1) Focus Ratio (FR): The proportion of Significant Memory and Significant Ignoring across all time steps. A higher FR indicates stronger selectivity.

$$FR = \frac{N_{SM} + N_{SI}}{N_{SM} + N_{SI} + N_{NR}} \tag{5}$$

2) Memory Entropy (ME): The entropy of all memory scores, where higher ME indicates stronger selectivity.

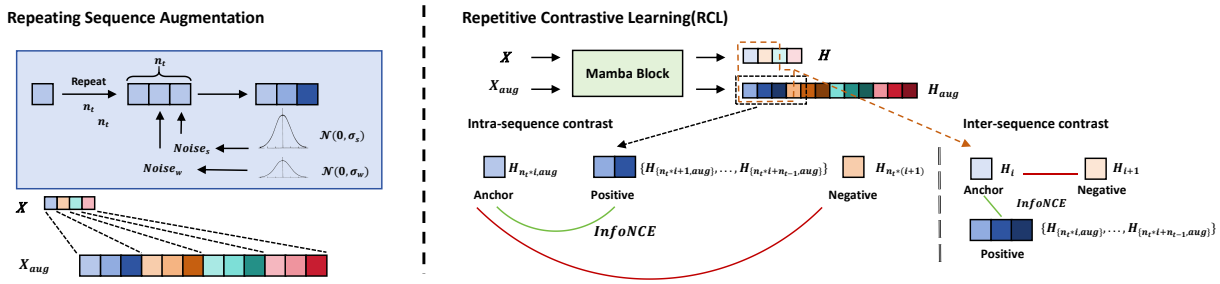

Figure 3: Process of the proposed method. Including Repeating Sequence Augmentation and Repetitive Contrastive Learning (RCL), with RCL consisting of Intra-sequence contrast and Inter-sequence contrast.

3. Method

The Repetitive Contrastive Learning (RCL) paradigm is a pretraining method used before training the backbone model. It enhances the Mamba block's selective capabilities through initialization parameters, improving the backbone model's performance. RCL consists of three main steps. First, augmented data is created by repeating time steps and adding increasing noise, with positive and negative sample pairs defined at the time-step level. Second, intra-sequence and inter-sequence contrastive learning is applied to a single Mamba block. Intra-sequence learning helps the model ignore noisy time steps and focus on meaningful ones, while inter-sequence learning ensures robust temporal feature modeling and consistency across sequences of different lengths. Finally, the pretrained parameters are used to initialize all Mamba blocks in the backbone model. RCL only requires pretraining once on a single Mamba block but can be applied universally to all Mamba-based models as an initialization strategy. This method is efficient and scalable, adding no extra memory overhead and minimal time cost.

3.1. Repeating Sequence Augmentation

One significant reason why Mamba performs exceptionally well in time series prediction tasks is its selective structure. To enhance the selection capability of the Mamba Block, we designed the Repeating Sequence Augmentation. Specifically, as shown in Fig. 3, for each time step in each time series, we sequentially repeat this time step with repetition count n_t.

$$\begin{aligned} \mathbf{X}_i &\xrightarrow{\text{repeat}} \mathbf{X}_{i,1}, ..., \mathbf{X}_{i,n_t} \\ \mathbf{X}_{\text{rep}} = \{&\mathbf{X}_{1,1}, ..., \mathbf{X}_{1,n_t}, ..., \mathbf{X}_{i,1}, ..., \\ &\mathbf{X}_{i,n_t}, ..., \mathbf{X}_{s,1}, ..., \mathbf{X}_{s,n_t}\} \end{aligned} \tag{6}$$

where $\mathbf{X}_i$ is the i-th step in time sequence, and s is the length of the sequence. For the time series $\mathbf{X} \in \mathbb{R}^{T\times F}$, $s = T$, the corresponding $\mathbf{X}_{\text{rep}} \in \mathbb{R}^{(n_t * T)\times F}$. As for inverted time series $\mathbf{X}^I \in \mathbb{R}^{F\times T}$, $s = F$, the corresponding $\mathbf{X}^I_{\text{rep}} \in \mathbb{R}^{(n_t * F)\times T}$.

Then, we add Gaussian noise of increasing intensity, from weak to strong, to the repeated time steps. In our experiments, we choose $n_t = 3$, each time step X_i is repeated and obtain $\mathbf{X}_{i,1}, \mathbf{X}_{i,2}, \mathbf{X}_{i,2}$. We then sample a strong Gaussian noise and a weak Gaussian noise, and add them to the repeated time steps in increasing order of intensity, from weak to strong.

$$\begin{aligned} \text{Noise}_\alpha &\sim \mathcal{N}(0, \sigma_\alpha^2) \\ \text{Noise}_\beta &\sim \mathcal{N}(0, \sigma_\beta^2) \\ \sigma_\alpha &< \sigma_\beta \\ \hat{\mathbf{X}}_{i,2} &= \mathbf{X}_{i,2} + \text{Noise}_\alpha \\ \hat{\mathbf{X}}_{i,3} &= \mathbf{X}_{i,3} + \text{Noise}_\beta \\ \mathbf{X}_{\text{aug},i} &= \{\mathbf{X}_{i,1}, \hat{\mathbf{X}}_{i,2}, \hat{\mathbf{X}}_{i,3}\} \\ \mathbf{X}_{\text{aug}} &= \mathbf{X}_{\text{aug},1} || \mathbf{X}_{\text{aug},2} || \ldots || \mathbf{X}_{\text{aug},s} \end{aligned} \tag{7}$$

where Noise_α and Noise_β represent weak and strong Gaussian noise, controlled by the variances σ_α and σ_β, $\|$ denotes the sequential concatenation of sequences. Since the impact of noise accumulates progressively during sequence modeling, gradually increasing the noise effectively amplifies the distance between time steps. As a result, the repeated time steps form a sequence of denoising targets with progressively increasing difficulty.

3.2. Repetitive Contrastive Learning

We input both the original sequence $\mathbf{X}$ and its augmented version $\mathbf{X}_{\text{aug}}$ into the same Mamba Block, comparing their respective outputs $\mathbf{H}$ and $\mathbf{H}_{\text{aug}}$ to evaluate the Mamba Block's modeling capabilities across both sequences. As illustrated in Fig.3, Repetitive Contrast Learning (RCL) encompasses two types of comparisons: intra-sequence contrast and inter-sequence contrast. Firstly, we define the output at any time step i with a repetition count n_t of the original sequence $\mathbf{X}_i$ as $\mathbf{H}_i$, and the output at the subsequent time step as $\mathbf{H}_{i+1}$. The outputs of the augmented sequence are represented as $\{\mathbf{H}_{\{i\cdot n_t,\text{aug}\}}, \mathbf{H}_{\{i\cdot n_t+1,\text{aug}\}}, \ldots, \mathbf{H}_{\{i\cdot n_t+n_t-1,\text{aug}\}}\}$, while the output at the next time step is $\{\mathbf{H}_{\{(i+1)\cdot n_t,\text{aug}\}}, \mathbf{H}_{\{(i+1)\cdot n_t+1,\text{aug}\}}, \ldots, \mathbf{H}_{\{(i+1)\cdot n_t+n_t-1,\text{aug}\}}\}$.

Intra-sequence contrast We hypothesize that if the Mamba Block possesses strong sequence selection capabilities, then the outputs $\{\mathbf{H}_{\{i\cdot n_t,\text{aug}\}}, \mathbf{H}_{\{i\cdot n_t+1,\text{aug}\}}, \ldots, \mathbf{H}_{\{i\cdot n_t+n_t-1,\text{aug}\}}\}$ of the augmented sequence at the same time step should exhibit high similarity, while ignoring progressively increasing noise. Conversely, the outputs $\mathbf{H}_{\{i\cdot n_t,\text{aug}\}}$ at the current time step and $\mathbf{H}_{\{(i+1)\cdot n_t,\text{aug}\}}$ at the subsequent time step should have low similarity. Therefore, we define outputs at the same time step as positive examples, while outputs at the current and subsequent time steps serve as negative examples. The objective is to minimize the distance between positive examples and maximize the distance between negative examples within the sequence, thereby enhancing the Mamba Block's sequence selection capabilities. Specifically, we use $\mathbf{H}_{\{i\cdot n_t,\text{aug}\}}$ as an anchor to form $n_t - 1$ positive samples and one negative sample, measuring similarity between samples using cosine similarity and employing the InfoNCE loss function Oord et al. (2018).

$$\mathcal{L}_{\text{Intra}} = -\frac{1}{s-1}\sum_{i=0}^{s-2}\frac{1}{n_t-1}\sum_{z=1}^{n_t-1}\log\frac{\exp(\text{sim}(\mathbf{H}_{\{i\cdot n_t,\text{aug}\}}, \mathbf{H}_{\{i\cdot n_t+z,\text{aug}\}})/\tau)}{\exp(\text{sim}(\mathbf{H}_{\{i\cdot n_t,\text{aug}\}}, \mathbf{H}_{\{(i+1)\cdot n_t,\text{aug}\}})/\tau)} \tag{8}$$

where s is the sequence length, i is the time step index, n_t is the repetition count, τ is a temperature coefficient controlling the distinction of negative samples, and $\text{sim}(\cdot,\cdot)$ denotes the cosine similarity function, defined as:

$$\text{sim}(h_i, h_j) = \frac{h_i \cdot h_j}{\|h_i\|\|h_j\|} \tag{9}$$

Intra-sequence contrast allows the Mamba Block to disregard noisy, repetitive time steps while prioritizing meaningful and effective ones, thereby strengthening its selection capabilities and noise resilience.

Inter-sequence contrast The inter-sequence contrast further enhances contrastive learning effects while preserving selection capability and temporal correlations on the original sequence, ensuring that the Mamba Block does not overfit to augmented data. Here, $\{\mathbf{H}_{\{i\cdot n_t,\text{aug}\}}, \mathbf{H}_{\{i\cdot n_t+1,\text{aug}\}}, \ldots, \mathbf{H}_{\{i\cdot n_t+n_t-1,\text{aug}\}}\}$ and $\mathbf{H}_i$ are defined as positive samples since they both represent the same time step and should maintain consistency across different time series lengths. Simultaneously, $\mathbf{H}_i$ and $\mathbf{H}_{i+1}$ are defined as negative samples to maintain selection capability on the original sequence.

$$\mathcal{L}_{\text{Inter}} = -\frac{1}{s-1}\sum_{i=0}^{s-2}\frac{1}{n_t}\sum_{z=0}^{n_t-1}\log\frac{\exp(\text{sim}(\mathbf{H}_i, \mathbf{H}_{\{i\cdot n_t+z,\text{aug}\}})/\tau)}{\exp(\text{sim}(\mathbf{H}_i, \mathbf{H}_{i+1})/\tau)} \tag{10}$$

where s, i, n_t, τ, and $\text{sim}(\cdot,\cdot)$ are defined as above.

The overall optimization objective for Repetitive Contrastive Learning is:

$$\mathcal{L}_{\text{rc}} = \mathcal{L}_{\text{Intra}} + \mathcal{L}_{\text{Inter}} \tag{11}$$

It is noteworthy that the pre-training process for Repetitive Contrastive Learning is conducted exclusively on a single Mamba Block rather than the entire Mamba model. Even when sequence length is repeated, the memory usage and training time are typically lower than what is required for the entire model.

3.3. Replace and Freezing Method

After repetitive contrastive learning, we obtain Mamba block parameters with enhanced selective capabilities. We use these parameters as the initialization parameters for the Mamba blocks in various Mamba-based backbone models, replacing the original initialization method to improve the temporal prediction performance of them.

Backbone models typically contain multiple Mamba blocks. We can choose to replace the initialization parameters for all blocks or only for a subset of them. The initialization parameters for other structures in the model, such as MLPs and attention mechanisms, remain unchanged. After parameter substitution, we can opt for full fine-tuning or partial fine-tuning of the replaced parameters. As discussed in Section 2.3, the selectivity of the Mamba block stems from the matrices $\mathbf{A}$, $\mathbf{B}$, and Δ, where only $\mathbf{A}$ is a globally optimizable matrix that encapsulates the common selective capabilities across all sequences. Therefore, in addition to full parameter fine-tuning, we recommend experimenting with freezing matrix $\mathbf{A}$ to preserve the learned selective capabilities.

Different parameter substitution and freezing methods may yield varying effects across different tasks. In Section 4.7, we analyze the impact of different substitution ratios and freezing methods using a four-layer Mamba as an example.

4. Experiment

We conducted extensive experiments to validate the effectiveness of our method. In Section 4.2, we compare the prediction performance of various Mamba-based models—Mamba (Gu and Dao, 2024), iMamba, TimeMachine (Ahamed and Cheng, 2024), Bi-Mamba (Liang et al., 2024) and SiMBA(Patro and Agneeswaran, 2024)—both with and without pre-trained parameters across multiple datasets: ETTh1, ETTh2, ETTm1, ETTm2, Traffic, and Electricity.

In Section 4.1, we provide an overview of the experimental setup and basic information. In Section 4.2, we demonstrate the performance improvement of the backbone model achieved by RCL. In Section 4.3, we compare RCL with other pretraining methods. In Section 4.4, we present the ablation study results of RCL. In Section 4.5, we analyze the impact of RCL parameters. In Section 4.6, we compare RCL with other temporal prediction models and achieve state-of-the-art results. In Section 4.7, we examine the effects of different parameter substitution ratios and freezing methods. Additionally, in Appendix B, we list additional experimental results.

4.1. Basic Information

4.1.1. Mamba-based Baseline

- **Mamba** (Gu and Dao, 2024): Mamba is a new Selective State Spaces model proposed by Albert Gu and Tri Dao in 2024.(Li et al., 2024) It demonstrates outstanding performance in sequence modeling through its selective state space formulation, effectively capturing long-range dependencies while maintaining computational efficiency.

- **iMamba**: An enhancement of Mamba, iMamba builds upon the principles of the iTransformer, where features are treated as tokens. This model is tailored specifically for time series forecasting tasks, offering improved flexibility in feature tokenization.

- **TimeMachine** (Ahamed and Cheng, 2024): TimeMachine, introduced by Md Atik Ahamed and Qiang Cheng in 2024, is designed for long-term sequence forecasting. By integrating channel-independent and channel-mixed modeling approaches, it achieves state-of-the-art performance. The architecture incorporates four Mamba blocks, optimizing predictive capability over extended sequences.

- **Bi-Mamba** (Liang et al., 2024): Bi-Mamba was proposed in 2024, Bi-Mamba extends the Mamba framework by adaptively capturing both internal and inter-series dependencies in multivariate time series data. The model introduces forget gates, enabling it to retain relevant historical information over extended time periods, thereby enhancing its forecasting accuracy.

- **SiMBA** (Patro and Agneeswaran, 2024): SiMBA is a hybrid architecture that combines Mamba-based sequence modeling with EinFFT, a novel FFT-based channel mixer. It is designed to overcome Mamba's instability when scaling, offering a stable and efficient solution for large-scale sequence tasks. SiMBA refines selective state space models for improved scalability and performance in visual recognition. Due to space limitations, we omitted experiments whose output length longer than 96 for the SiMBA model.

4.1.2. Temporal Baseline

- **Transformer**: (Vaswani et al., 2023) The Transformer model, introduced by Vaswani et al. in 2017, revolutionized sequence modeling by using self-attention mechanisms. Its architecture allows for efficient parallelization and effectively captures long-range dependencies, making it highly suitable for various tasks such as natural language processing and time series forecasting.

- **iTransformer**:(Liu et al., 2024) iTransformer is a restructured Transformer tailored for multivariate time series forecasting. Instead of embedding simultaneous time steps, it encodes each variate's full time series as a token, enabling better capture of global patterns and cross-variate correlations. This design aligns attention with the intrinsic structure of time series and achieves strong performance across forecasting benchmarks.

- **TimeMixer**: (Wang et al., 2024) TimeMixer is a novel approach designed for time series modeling, leveraging the power of mixing operations to combine temporal features. By focusing on capturing intricate temporal dependencies and interactions, TimeMixer provides robust performance in both short-term and long-term forecasting tasks.

- **N-Beats**: (Oreshkin et al., 2020) N-Beats is a deep learning architecture designed for univariate time series forecasting. It employs a *Doubly Residual Stacking* mechanism, utilizing both backward and forward residual links to enhance signal propagation through a deep stack of fully connected layers. The model is highly flexible, requiring no time-series-specific components, and demonstrates state-of-the-art performance across diverse datasets, including M3, M4, and TOURISM. Additionally, N-Beats incorporates *Ensembling* techniques during training, further improving its robustness and accuracy.

- **N-HiTS**: (Challu et al., 2022) N-HiTS builds upon N-Beats by introducing a *Neural Basis Approximation Theorem* to enhance theoretical guarantees in forecasting. The model significantly improves long-horizon predictions through *Multi-Rate Signal Sampling*, allowing it to focus on different frequency components dynamically. Additionally, N-HiTS employs a *Hierarchical Interpolation* mechanism, which enables efficient decomposition and synthesis of forecasted signals, reducing volatility and computational complexity.

- **CrossFormer**: (Wang et al., 2021) CrossFormer introduces a cross-attention mechanism specifically tailored for time series data. It excels in integrating multiple time series inputs, enabling the model to learn complex relationships across different temporal sequences, thus improving forecasting accuracy and adaptability to diverse datasets.

- **PatchTST**: (Nie et al., 2023) PatchTST is a model that applies the concept of patch-based processing from computer vision to time series data. By segmenting time series into patches and processing them independently, PatchTST enhances the model's ability to capture local temporal patterns, improving efficiency and scalability for large datasets.

- **TimesNet**: (Wu et al., 2023) TimesNet is an advanced time series network that leverages a hierarchical structure to model temporal dependencies at multiple scales. This architecture allows TimesNet to adaptively focus on different temporal resolutions, providing superior performance in multiscale time series forecasting.

- **FEDFormer**: (Zhou et al., 2022) FEDFormer incorporates federated learning principles into the Transformer framework, allowing for decentralized time series modeling. This model is particularly effective in scenarios where data privacy is crucial, as it can learn from distributed data sources without centralizing the datasets.

- **Informer**: (Zhou et al., 2021) Informer is designed to efficiently handle long sequences in time series forecasting. It introduces a ProbSparse self-attention mechanism that reduces computational complexity and memory usage, making it ideal for real-time applications and large-scale datasets. Informer achieves state-of-the-art results by focusing on significant temporal patterns while filtering out noise.

4.1.3. Temporal Pre-training Baseline

- **SoftCLT**: (Lee et al., 2024) SoftCLT is a cutting-edge model designed for contextual sequence learning. By incorporating soft clustering techniques, SoftCLT dynamically groups similar temporal patterns, enhancing the model's ability to generalize across varied contexts. This approach ensures superior performance in complex classification tasks, offering robust adaptability to fluctuating sequences while maintaining high interpretability.

- **InfoTS**: (Luo et al., 2023) InfoTS leverages information-theoretic principles to optimize time series modeling. By prioritizing the retention of informative features and minimizing redundancy, InfoTS significantly enhances predictive accuracy. This model excels in both supervised and unsupervised learning scenarios, making it versatile for diverse applications such as anomaly detection and trend analysis.

4.1.4. Dataset

Frequency, number of features, and time point information of the datasets.

Dataset	Frequency	Features	Time Points	Split
ETTh1	Hour	7	17420	60%/20%/20%
ETTh2	Hour	7	17420	60%/20%/20%
ETTm1	15 Minutes	7	69680	60%/20%/20%
ETTm2	15 Minutes	7	69680	60%/20%/20%
Traffic	Hour	862	17544	60%/20%/20%
Electricity	Hour	321	26304	60%/20%/20%

4.1.5. Metric

Mean Absolute Error (MAE):

$$\text{MAE} = \frac{1}{n}\sum_{i=1}^{n}|y_i - \hat{y}_i|$$

Mean Squared Error (MSE):

$$\text{MSE} = \frac{1}{n}\sum_{i=1}^{n}(y_i - \hat{y}_i)^2$$

4.1.6. Model Settings

The parameter settings for the Mamba block during pre-training are as follows: The model dimension (d_{model}) is set to values [16, 32, 64], and the state dimension (d_{state}) is set to [16, 64, 128]. The convolution dimension (d_{conv}) is fixed at 4, and $pad_vocab_size_multiple$ is set to 8 to ensure consistent padding sizes. The expansion factor ($expand$) is configured to 2, with $conv_bias$ enabled (set to True) and $bias$ disabled (set to False). The repeat time, denoted as n_t, is set to 3, while noise variance is varied between [0.001, 0.01]. During the inference phase, the Mamba Selective State Space Model (SSM) parameters are aligned with the corresponding pre-trained block parameters to maintain consistency and leverage learned patterns effectively.

4.1.7. Training Settings

The experiment was conducted on a server equipped with four NVIDIA GeForce RTX 3090 GPUs and an AMD EPYC 7282 16-Core Processor. During the pre-training phase, the number of layers (n_layer) is set to 1, the number of epochs ($epoch$) is 100, the learning rate (lr) is configured to 1e-4, and the regularization coefficient is also set to 1e-4. In the inference stage, the maximum number of training epochs remains at 100, while n_layer is increased to 4. The Mean Absolute Error (MAE) serves as the loss function, and model selection is based on the lowest validation set loss. The parameter $frozentype$ is chosen as needed from the options [None, FrozenA], and the number of layers used for parameter replacement is selected from [25%, 50%, 75%, 100%], according to the specific experimental requirements. For the prediction length, we selected four different lengths: [96, 192, 336, 720] and conducted a series of experiments. However, all results tables presented in our paper, unless otherwise specified, use a prediction length of 96. This length was chosen because it effectively illustrates the corresponding conclusions and provides a clear basis for our findings.

4.2. Main Result

		ETTh1		ETTh2		ETTm1		ETTm2		Traffic		Electricity	
		MAE	MSE	MAE	MSE	MAE	MSE	MAE	MSE	MAE	MSE	MAE	MSE
Mamba	w/o	0.6546	0.7672	1.4013	2.8442	0.5053	0.5432	0.5763	0.6008	0.4939	1.0279	0.4232	0.3926
	w	0.5974	0.6542	1.1536	2.0506	0.4798	0.4946	0.5646	0.5677	0.4604	0.9076	0.4168	0.3879
	up-rate%	**8.7382**	**14.729**	**17.676**	**27.902**	**5.0465**	**8.9470**	**2.0302**	**5.5093**	**6.7827**	**11.704**	**1.5123**	**1.1971**
iMamba	w/o	0.4987	0.4928	0.6926	0.9084	0.4316	0.3998	0.4160	0.3666	0.3234	0.6538	0.2627	0.1857
	w	0.4472	0.4278	0.6833	0.8595	0.3970	0.3669	0.3304	0.2469	0.2913	0.6003	0.2597	0.1827
	up-rate%	**10.327**	**13.190**	**1.3428**	**5.3831**	**8.0167**	**8.2291**	**20.577**	**32.651**	**9.9258**	**8.1829**	**1.1420**	**1.6155**
TimeMachine	w/o	0.3905	0.3833	0.3344	0.2911	0.3606	0.3342	0.2525	0.1746	0.3064	0.4983	0.2611	0.1872
	w	0.3869	0.3787	0.3298	0.2822	0.3458	0.3179	0.2508	0.1731	0.2991	0.4844	0.2586	0.1826
	up-rate%	**0.9219**	**1.2001**	**1.3756**	**3.0574**	**4.1043**	**4.8773**	**0.6733**	**0.8591**	**2.3825**	**2.7895**	**0.9575**	**2.4573**
Bi-Mamba	w/o	0.3948	0.3813	0.3494	0.3073	0.3641	0.3319	0.2704	0.1883	0.2786	0.587	0.2629	0.185
	w	0.3893	0.3794	0.3472	0.3	0.3578	0.3316	0.2707	0.1857	0.2761	0.5787	0.2611	0.1818
	up-rate%	**1.3931**	**0.4983**	**0.6297**	**2.3755**	**1.7302**	**0.0903**	-0.1109	**1.3808**	**0.8973**	**1.4140**	**0.6847**	**1.7280**
SiMBA	w/o	0.4206	0.4033	0.4097	0.3643	0.3841	0.3466	0.2801	0.1900	0.2601	0.5416	0.2433	0.1531
	w	0.4109	0.3899	0.3817	0.3238	0.3742	0.3391	0.2764	0.1868	0.2566	0.5404	0.2412	0.1527
	up-rate%	**2.2966**	**3.3153**	**6.8481**	**11.136**	**2.5720**	**2.1853**	**1.3149**	**1.6561**	**1.3315**	**0.2233**	**0.8496**	**0.3117**

Table 1: Comparison of performance improvement by replacing parameters obtained by RCL. w/o denotes no parameter replacement, w denotes parameter replacement, and up-rate represents the improvement rate.

We validated the performance improvements brought by the parameters of the pre-trained Mamba block across multiple Mamba-based models, as shown in Table 1. By leveraging the pre-trained Mamba block parameters, the Mamba model demonstrated substantial gains across various datasets, with the Mean Squared Error (MSE) reduced by up to 27.9% and the Mean Absolute Error (MAE) improved by up to 17.7%, averaging an improvement of over 5%. For the iMamba model, the MAE showed gains of up to 20.6%, while the MSE improved by up to 32.7%, with an average performance increase exceeding 8%. These results indicate that the Mamba block parameters, refined through Repetitive Contrastive Learning, significantly enhance the predictive capabilities of the Mamba and iMamba models in time series tasks, yielding average improvements of 5% to 8%.

For the TimeMachine model, MSE improved by up to 4.88% and MAE by up to 4.10%, with an average improvement of 2%. While these gains are smaller compared to the Mamba and iMamba models, they remain noteworthy given that Bi-Mamba, SiMBA and TimeMachine are already state-of-the-art models for long-term sequence prediction. Achieving an additional 1% to 2% improvement solely by replacing the Mamba block parameters represents a meaningful advancement.

In summary, the parameters of the Mamba block, learned through the Repetitive Contrastive Learning method, consistently enhance the performance of various Mamba-based models. This underscores our method's efficacy in improving the sequence selection capability of the Mamba block and highlights its adaptability and potential for broad application.

4.3. Comparison with Pre-training Methods

We conducted a series of experiments on the latest pre-training methods in the time series domain (Luo et al., 2023; Lee et al., 2024). The results, presented in Table 2, were derived from models trained using official code on multivariate forecasting tasks. Two important aspects warrant attention. First, both methods are designed to enhance the representation learning of time series features through contrastive pre-training, heavily relying on the capabilities of feature extraction modules. Specifically, their experiments utilized the TSEncoder from woTS2Vec(Yue et al., 2022) or TC from CATCC(Eldele et al., 2023) as feature extractors. These models are structurally distinct from mamba-based models, leading to a decline in performance when feature extraction is adapted to mamba models. Second, these approaches primarily benefit classification tasks due to their ability to accurately and effectively represent time series nodes, which aids classification but demonstrates limited improvements in forecasting tasks especially in multivariate tasks. Consequently, during their prediction stages, they use feature vectors from pre-training train a linear model to predict future values instead of leveraging pre-trained modules to construct new models. In contrast, our pre-training approach guides mamba blocks to learn sampling rules inherent in natural time sequences and identify

Model		**TimeMachine***		**Bi-Mamba***		**Mamba***		**iMamba***		InfoTS(TS2Vec)		SoftCLT(TS2Vec)		SoftCLT(Mamba)		InfoTS(Mamba)	
Metric		MAE	MSE	MAE	MSE	MAE	MSE	MAE	MSE	MAE	MSE	MAE	MSE	MAE	MSE	MAE	MSE
ETTh1	96	**0.387**	**0.379**	0.389	0.379	0.575	0.657	0.499	0.493	0.623	0.736	0.616	0.704	0.696	0.891	0.816	1.147
	192	**0.420**	0.440	0.421	**0.425**	0.602	0.713	0.508	0.532	0.690	0.857	0.670	0.810	0.737	0.959	0.835	1.186
	336	**0.442**	0.482	0.456	**0.481**	0.608	0.715	0.513	0.550	0.769	1.024	0.740	0.950	0.640	1.064	0.861	1.231
ETTh2	96	**0.330**	**0.282**	0.347	0.300	1.228	2.124	0.693	0.908	0.754	0.936	0.799	1.015	0.997	1.542	0.897	1.219
	192	**0.382**	**0.355**	0.394	0.373	1.237	2.164	1.023	1.821	1.112	2.022	1.251	2.559	1.343	2.820	1.251	2.506
	336	**0.420**	**0.412**	0.429	0.434	1.234	2.153	1.073	2.042	1.264	2.482	1.312	2.639	1.402	2.952	1.327	2.733
ETTm1	96	**0.346**	**0.318**	0.358	0.332	0.492	0.528	0.432	0.400	0.540	0.602	0.534	0.581	0.623	0.808	0.741	0.985
	192	**0.377**	0.375	0.384	**0.369**	0.513	0.587	0.450	0.439	0.575	0.649	0.569	0.635	0.654	0.849	0.756	1.014
	336	**0.387**	**0.396**	0.407	0.404	0.817	1.457	0.491	0.509	0.622	0.729	0.610	0.697	0.681	0.885	0.770	1.040
ETTm2	96	**0.251**	**0.173**	0.271	0.186	0.576	0.601	0.416	0.367	0.452	0.377	0.460	0.400	0.491	0.437	0.782	0.969
	192	**0.293**	**0.238**	0.313	0.254	0.667	0.847	0.497	0.495	0.560	0.542	0.580	0.587	0.591	0.590	0.857	1.152
	336	**0.333**	**0.299**	0.364	0.316	0.705	0.922	0.793	1.032	0.713	0.846	0.730	0.885	0.730	0.855	0.969	1.461
Electricity	96	**0.259**	0.183	0.261	**0.182**	0.423	0.393	0.260	0.183	0.290	0.380	0.401	0.326	0.553	0.571	0.531	0.524
	192	**0.246**	**0.152**	0.270	0.188	0.430	0.405	0.280	0.205	0.293	0.383	0.403	0.327	0.555	0.573	0.532	0.524
	336	**0.261**	**0.169**	0.283	0.200	0.435	0.411	0.298	0.222	0.311	0.396	0.416	0.344	0.565	0.581	0.540	0.538

Table 2: Comparison results with pre-training methods. Bolded names with an asterisk indicate models using our pre-training methods. Parentheses following InfoTS and SoftCLT denote the backbone models utilized during pre-training. The best results for each metric are highlighted in bold.

meaningful historical information. This aligns with the requirements of forecasting tasks, allowing us to directly leverage parameters in forecasting models for superior results.

Model	**ETTh1**		**ETTh2**		**ETTm1**		**ETTm2**		**Traffic**		**Electricity**	
Metric	MAE	MSE	MAE	MSE	MAE	MSE	MAE	MSE	MAE	MSE	MAE	MSE
TimeMachine*	**0.429**	0.447	**0.390**	**0.365**	**0.385**	0.386	**0.317**	0.278	0.287	0.446	**0.265**	**0.176**
TimeMachine	0.432	0.452	0.397	0.376	0.391	0.395	0.319	0.282	0.290	0.454	0.269	0.181
Bi-Mamba*	0.441	0.445	0.443	0.460	0.398	0.391	0.340	0.290	0.308	0.640	0.283	0.206
Bi-Mamba	0.445	0.452	0.445	0.459	0.404	0.395	0.351	0.317	0.307	0.644	0.287	0.212
iTransformer	0.448	0.454	0.407	0.383	0.410	0.407	0.332	0.288	**0.282**	**0.428**	0.270	0.178
TimeMixer	0.440	0.447	0.395	0.365	0.396	**0.381**	0.323	**0.275**	0.298	0.485	0.273	0.182
CrossFormer	0.522	0.529	0.684	0.942	0.495	0.513	0.611	0.757	0.304	0.550	0.334	0.244
PatchTST	0.455	0.469	0.407	0.387	0.400	0.387	0.326	0.281	0.362	0.555	0.304	0.216
TimesNet	0.450	0.458	0.427	0.414	0.406	0.400	0.333	0.291	0.336	0.620	0.295	0.193
FEDFormer	0.460	**0.440**	0.449	0.437	0.452	0.448	0.349	0.305	0.376	0.610	0.327	0.214
Informer	0.795	1.040	1.729	4.431	0.734	0.961	0.810	1.410	0.397	0.311	0.416	0.764
N-HiTS	0.455	0.475	0.448	0.421	0.416	0.410	0.330	0.279	0.311	0.452	0.329	0.246
N-BEATS	0.488	0.490	0.471	0.411	0.401	0.418	0.345	0.294	0.321	0.461	0.329	0.246

Table 3: Comparison results with temporal model. Bolded numbers indicate optimal results and underscores indicate sub-optimal results.

4.4. Ablation Study

We conducted two ablation experiments to evaluate our proposed RCL method. All ablation experiments used a 4-layer Mamba as the baseline model. In the first ablation experiment, as shown in Table 4, we separately removed intra-sequence contrast, inter-sequence contrast, and noise. Removing intra-sequence contrast significantly reduced prediction performance because this contrast enhances the Mamba block's ability to select time steps and denoise. Without it, the model's ability to select time steps diminishes. Similarly, removing inter-sequence contrast also led to performance loss, as repeated time sequences can disrupt temporal consistency. The purpose of inter-sequence contrast is to maintain consistency with the temporal features of the original sequence. Without it, RCL cannot learn temporal features in broken sequences. The most significant performance drop occurred when noise was removed. Without added noise, repeated time steps are indistinguishable from the original ones, reducing task difficulty and failing to enhance the Mamba block's ability to resist noise and select time steps.

	ETTh1		ETTh2	
	MAE	MSE	MAE	MSE
w/o intra-sequence contrast	0.636	0.743	1.351	2.659
w/o inter-sequence contrast	0.622	0.710	1.296	2.421
w/o noise	0.655	0.767	1.401	2.844
our approach	**0.597**	**0.654**	**1.154**	**2.051**

Table 4: Ablation results for our contrastive method settings, highlighting the effects of intra-sequence, inter-sequence, and noise augmentation components, which correspond to the three key parts of our model design.

	ETTh1		ETTh2	
	MAE	MSE	MAE	MSE
RCL w uniform noise	0.601	0.664	1.158	2.060
RCL w constant-intensity Gaussian noise	0.600	0.660	1.155	2.059
RCL w increasing-intensity Gaussian noise	**0.597**	**0.654**	**1.154**	**2.051**

Table 5: Ablation study on the design of increasing-intensity Gaussian noise. We conducted a series of explorations examining different noise formats and their impact.

In the second ablation experiment, as shown in Table 5, we compared the effects of different types of noise on performance. Specifically, we compared uniform noise, constant-intensity Gaussian noise, and increasing-intensity Gaussian noise used in RCL. All three types of noise yielded good results, with uniform noise performing slightly worse than constant-intensity Gaussian noise, and constant-intensity Gaussian noise performing slightly worse than increasing-intensity Gaussian noise. The increasing-intensity Gaussian noise further accentuates differences between repeated time steps, increasing the difficulty of distinguishing effective information from noise, thereby enhancing pre-training performance.

4.5. Hyper-Parameter Experiment of RCL

n_t	ETTh1		ETTh2	
	MAE	MSE	MAE	MSE
2	0.623	0.708	1.182	2.145
3	**0.597**	**0.654**	**1.154**	**2.051**
4	0.591	0.653	1.148	2.003

σ_a	ETTh1		ETTh2	
	MAE	MSE	MAE	MSE
5e-4	0.614	0.671	1.180	2.085
1e-3	**0.597**	**0.654**	**1.154**	**2.051**
5e-3	0.601	0.700	1.172	2.072
1e-2	0.629	0.683	1.199	2.096

Table 6: RCL Parameter Experiment Results

	SM	SF	Normal	Focus ratio	ME
w RCL	11897	32789	219889	0.1689	1.53
w/o RCL	5641	12875	246059	0.0700	1.04

Table 7: Focus Ratio and Memory Entropy

We conducted experimental comparisons on the RCL training parameters. Specifically, we compared different repetition counts n_t and initial noise intensities σ_a. We set the noise intensity for each repetition is twice that of the previous one. The experimental results are shown in Table 5. It can be observed that when $n_t = 2$, the performance is significantly lower than others. This is because fewer repetitions make the task simpler and do not significantly enhance the original model. When $n_t = 4$, the performance is only slightly better than when $n_t = 3$. However, considering training time and memory usage, we believe that overall, $n_t = 3$ is preferable. Regarding the initial noise intensity σ_a, when $\sigma_a = 5 \times 10^{-3}$, the noise is relatively weak, causing low interference and making the task simpler, resulting in weaker performance improvement. When σ_a is greater than 1×10^{-3}, the noise becomes too strong, significantly differing from the original temporal signals, thus reducing the difficulty of recognition and leading to less performance improvement.

4.6. Comparison with Temporal Model

We compared our approach with existing state-of-the-art time series prediction models. We set all input lengths to 96 and conducted experiments across multiple prediction horizons $T = \{96, 192, 336, 720\}$. The average results across the four prediction horizons are presented in Table 3, while the detailed results for each individual prediction horizon are provided in Table B.10 of Appendix B.1. TimeMachine* and Bi-Mamba* refer to the TimeMachine and Bi-Mamba models initialized with parameters obtained using RCL. Our method achieves optimal results across various datasets and prediction horizons. For datasets with fewer data channels, our approach consistently achieves the best Mean Absolute Error (MAE) results across all prediction horizons, and Mean Squared Error (MSE) results are generally among the top two. For datasets with more channels, such as traffic and electricity, our method shows more significant improvements for longer prediction targets. This indicates enhanced stability in long-sequence predictions, attributed to the parameters obtained through RCL, which enable the Mamba block to have stronger selectivity for time series data.

4.7. Comparison of Replacement and Freezing Methods

		ETTm1				ETTm2			
		None		FrozenA		None		FrozenA	
		MAE	MSE	MAE	MSE	MAE	MSE	MAE	MSE
	w/o	0.5053	0.5432	0.5053	0.5432	0.5763	0.6008	0.5763	0.6008
layer-25%	w	0.4921	0.5394	0.4921	0.5393	0.6609	0.7902	0.5611	0.5696
	up-rate%	**2.6123**	**0.6996**	**2.6123**	**0.7180**	-14.6799	-31.5246	**2.6375**	**5.1931**
layer-50%	w	0.4798	0.4946	0.4976	0.5548	0.6021	0.6230	0.6389	0.7423
	up-rate%	**5.0465**	**8.9470**	**1.5238**	-2.1355	-4.4768	-3.6951	-10.8624	-23.5519
layer-75%	w	0.4816	0.5256	0.4816	0.5255	0.5299	0.5366	0.5646	0.5676
	up-rate%	**4.6903**	**3.2401**	**4.6903**	**3.2585**	**8.0514**	**10.6858**	**2.0302**	**5.5260**
layer-100%	w	0.5106	0.5692	0.5016	0.5658	0.5486	0.5735	0.5296	0.5258
	up-rate%	-1.0489	-4.7865	**0.7322**	-4.1605	**4.8065**	**4.5439**	**8.1034**	**12.4834**

Table 8: Comparison of Replacement and Freezing Methods. The "layer-x%" indicates that the first x% of layers were replaced by pre-trained blocks.

A Mamba-based model typically comprises multiple Mamba blocks. Each Mamba block contains a matrix **A**, which is defined in 3.2. The parameters are responsible for controlling the block's selectivity towards information before. To evaluate the impact of parameter replacement and parameter freezing during the inference stage, we used a 4-layer Mamba model as a baseline. The replacement strategy involved substituting 25%, 50%, 75%, and 100% of the Mamba blocks, while the parameter freezing strategy was categorized into no freezing (None) and freezing of matrix **A** (FrozenA). Freezing matrix **A** helps preserve the enhanced selectivity gained during pre-training.

As shown in Table 8, the optimal parameter replacement and freezing strategies differ across datasets. For the ETTm1 dataset, replacing 50% of the Mamba blocks without freezing any parameters yielded the greatest improvement, while replacing 100% of the blocks resulted in the lowest performance. This suggests that the selection capabilities of the pre-trained parameters do not fully align with the prediction target. By replacing only 50% of the Mamba blocks, the model can better encode the time series, while the remaining blocks focus on fitting the specific prediction requirements of the dataset, ultimately enhancing model performance.

Conversely, for the ETTm2 dataset, the greatest improvement was achieved by replacing all Mamba blocks and freezing matrix **A**. In this case, the selective enhancements from pre-training aligned well with the dataset's prediction targets. This approach preserved the pre-trained parameters' selectivity while allowing the remaining parameters to adjust to fit the prediction targets effectively.

Similar results were observed across other datasets. Broadly, the findings can be grouped into two effective strategies: replacing 50% of the Mamba blocks without freezing any parameters and replacing 100% of the Mamba blocks while freezing matrix **A**. We recommend choosing between these two approaches during the inference phase for optimal performance.

5. Analysis

5.1. Analysis of Time and Memory Overhead

Sequence repetition and Repetitive Contrastive Learning introduce additional memory and time overhead. To better understand the implications, we analyze the time and space complexity of the entire training process. The memory overhead for Mamba is determined by the number of blocks, n_b, and sequence length, s_l, yielding a complexity of $O(s_l n_b)$. During pre-training, only a single Mamba block is utilized, with input sequence lengths $n_t s$ and s, resulting in a space complexity of $O((n_t + 1)s)$. Meanwhile, the memory consumption during inference is represented as $O(sn_b)$. Table 9 details the memory consumption for Mamba training with $n_t = 3$ and $n_b = 4$ layers, illustrating that the peak memory overhead is comparable. As the number of Mamba layers increases, the memory requirement for pre-training remains significantly lower than that of the inference stage.

Due to Mamba's unique computational optimizations, the time complexity of a Mamba block is linear with respect to the sequence length s_l, denoted as $O(s_l)$. During pre-training, the sequence length is $n_t s$, whereas during inference, it is s. As such, the training time with pre-training is approximately $n_t + 1$ times longer compared to training without pre-training. Table 9 shows that when $n_t = 3$, the pre-training time consumption is about three times that of inference, which is consistent with our theoretical analysis.

	Memory(Unit: MB)			Time(Unit: S)		
ETTh1	Pretrain	Inference	Max Memory	Pretrain	Inference	Total
w/o	-	11733	11733	-	1.69	1.71
w	13131	11470	13131	5	1.62	6.54
Traffic	Pretrain	Inference	Max Memory	Pretrain	Inference	Total
w/o	-	1602	1602	-	2.67	2.68
w	1994	1298	1994	6	2.54	8.54

Table 9: Peak memory consumption and average time overhead. The batch size for the ETTh1 dataset is 2000, while for the Traffic dataset it is 100.

5.2. *Analysis of Enhanced Selectivity*

Through Focus Ratio and Memory Entropy

We compared the Focus Ratio and Memory Entropy of the Mamba block when modeling time series with and without RCL, and the results are shown in Table 6. It can be observed that after applying RCL, the Focus Ratio significantly improves, indicating more pronounced processes of significant memory and significant forgetting. This suggests that the model becomes more focused on key information and more decisive in ignoring noisy information. Similarly, RCL also leads to a notable increase in Memory Entropy, demonstrating that the Mamba block's memory patterns for time-step information become more complex and diverse. This enables the model to better capture essential aspects of the sequence with greater selectivity.

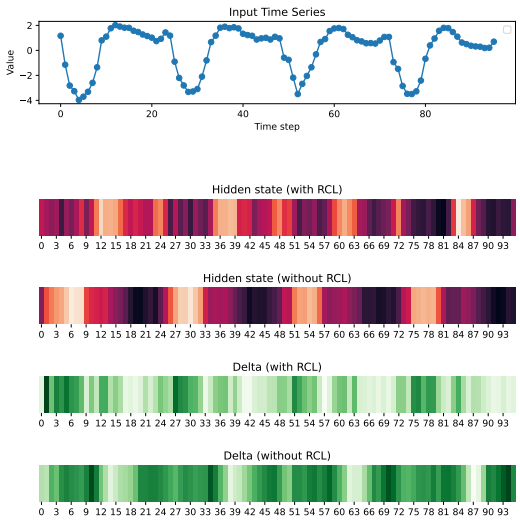

Figure 4: Hidden state and Δ corresponding to the input time series.

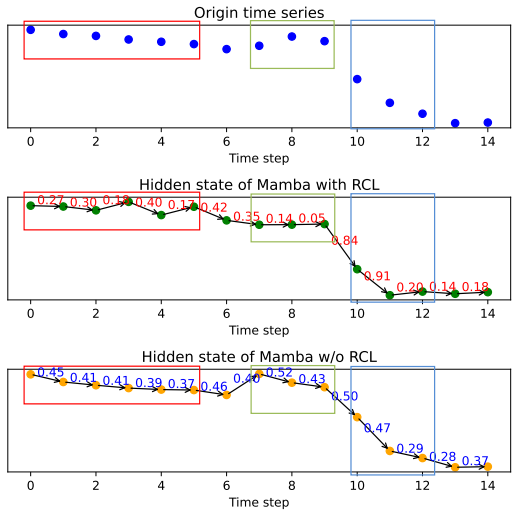

Figure 5: Memory and ignoring in Mamba models with and without RCL.

Through Visualization of the Hidden state and Delta

We demonstrate that our proposed RCL effectively enhances the time step selection capability of the Mamba block by visualizing the Hidden state and Delta corresponding to the input time series of the Mamba block. The visualization

results are shown in Figure 4. According to the principles of SSM, the Hidden state can be represented in a form similar to a recurrent neural network:

$$\mathbf{H}_{t+1} = \overline{\mathbf{A}}\mathbf{H}_t + \overline{\mathbf{B}}\mathbf{X}_{t+1} \tag{12}$$

The matrix **A** determines how historical temporal information is retained. In the Mamba block, the matrix $\overline{\mathbf{A}}$ is determined by a fixed matrix **A** and Δ, where **A** influences part of the historical information selection, and Δ influences another part. The visualization results indicate that without initializing with RCL parameters, the Hidden state is almost directly proportional to the input, and Δ is similarly proportional to the input. This suggests that directly training the Mamba block does not effectively retain historical information; the matrix **A** nearly forgets all historical information, retaining only the current information as the hidden state.

In contrast, when training with initialized parameters, the Hidden state exhibits more complex representations, and Δ shows a more intricate temporal pattern. This indicates that the model learns complex inter-dependencies between time steps. The matrix **A** learned by RCL demonstrates different memory and ignoring patterns for historical information across various time steps. It retains more of the input at critical time steps while preserving more historical information at non-critical time steps, thereby significantly enhancing the Mamba block's ability to select relevant information from time series data.

Through Visualization of Memory and Ignoring Processes We visualized the evolution of the memory score for a sequence when using RCL and when not using RCL, where the definition of the memory score is provided in Section 2.4.The visualization results are presented in Figure 5, where the numbers on the arrows indicate the memory weights for the previous time step. From the perspective of recurrent neural networks, it is evident that without using RCL for parameter initialization, the Mamba block maintains historical memory weights between 30% and 50% across all time steps, resulting in a hidden state that closely resembles the original time series. In contrast, the Mamba block with RCL exhibits a richer memory pattern, demonstrating significant noise resistance and strong memory retention for critical time steps.

In region (a) of Figure 5, the original time series is monotonically decreasing. Here, the hidden state of Mamba w/o RCL is almost identical to the original time series, while Mamba with RCL maintains the overall downward trend but differentiates the spatial representation of each time step, resulting in more pronounced changes in the hidden state. In region (b), a brief noise appears amidst the overall decline. Mamba w/o RCL is noticeably affected by this noise, whereas Mamba with RCL overcomes the noise interference by leveraging high historical memory weights. In region (c), the original time series experiences a significant drop. Mamba with RCL accurately identifies the critical points of this abrupt change, largely ignoring historical information to prominently incorporate the crucial time step information into the hidden state.

5.3. Theoretical Analysis of Repetitive Contrastive Learning

We conducted a theoretical analysis of RCL with a single repetition. For S4 SSM, where A and B are fixed, for any anchor h_t, the positive example is the time step after repetition $h_t^+ = Ah_t + B(x_t + \sigma)$, and the negative example is the next time step $h_t^- = Ah_t^+ + Bx_{t+1} = A^2h_t + AB(x_t + \sigma) + Bx_{t+1}$. We measure relevance using cosine similarity, assuming all vectors are normalized, so cosine similarity simplifies to $sim(a, b) = a \cdot b$.

$$\text{Sim}_{\text{pos}} = sim(h_t, h_t^+) = Ah_t^2 + B(x_t + \sigma)h_t$$

$$\text{Sim}_{\text{neg}} = sim(h_t, h_t^-) = A^2h_t^2 + AB(x_t + \sigma)h_t + Bx_{t+1}h_t$$

Assuming a temperature coefficient of 1, the contrastive loss can be written as:

$$\text{Loss} = \log(1 + \exp(\text{Sim}_{\text{neg}} - \text{Sim}_{\text{pos}}))$$

Minimizing the InfoNCE loss can be interpreted as maximizing the lower bound of mutual information between the anchor and the positive example(van den Oord et al., 2019; Wu et al., 2020):

$$I(h_t, h_t^+) \geq -\text{Loss} = -\log(1 + \exp(\text{Sim}_{\text{neg}} - \text{Sim}_{\text{pos}}))$$

This means making the representations of the noise-free and the next noisy time step similar. Essentially, Mamba aims to remove the interference of noisy time steps and maintain the hidden state unchanged.

Maximizing the lower bound of mutual information is equivalent to minimizing:

$$\mathrm{Sim}_{\mathrm{neg}} - \mathrm{Sim}_{\mathrm{pos}} = (A^2 - A)h_t^2 + (AB - B)(x_t + \sigma)h_t + Bx_{t+1}h_t$$

By taking derivatives with respect to A and B, we can solve for the optimal A^* and B^*:

$$A^* = \frac{h_t^2 - B(x_t + \sigma)h_t}{2h_t^2}$$

$$B^* = \frac{h_t(2x_{t+1} - x_t - \sigma)}{(x_t + \sigma)^2}$$

The optimal lower bound is:

$$-\log\left(1 + \exp\left(\frac{x_{t+1}^2 - x_{t+1}(x_t + \sigma)}{(x_t + \sigma)^2}h_t^2\right)\right)$$

As we gradually increase σ, the lower bound of mutual information continues to improve, indicating that S4's resistance to noise is enhanced. This is reflected in $h_t^+ = Ah_t + B(x_t + \sigma)$, where A tends to 1 and B tends to 0, emphasizing the selection of historical information while ignoring noisy time steps.

Furthermore, we analyze the state transition in Mamba. In Mamba, matrices A and B can be approximately considered as linearly transformed from the current time step:

$$A_+ = W_A(x_t + \sigma), \quad A_- = W_A x_{t+1}, \quad B_+ = W_B(x_t + \sigma), \quad B_- = W_B x_{t+1}$$

Substituting into the loss function and taking derivatives with respect to W_A and W_B, the optimal lower bound of mutual information is:

$$-\log\left(1 + \exp\left(\frac{h_t^2 x_{t+1}^4}{(x_t + \sigma)^3} + \frac{h_t^2}{x_t + \sigma}\right)\right)$$

An increase in noise intensity enhances the lower bound of mutual information, and the optimal lower bound is more sensitive to noise.

6. Visualization of Comparative Effects

6.1. Visualization of Embedding in Augmentation Sequence

To visually demonstrate the impact of our contrastive learning methods, we plotted the cosine similarity values(Rahutomo et al., 2012) between embedding vectors of the same input sequence from the ETTm1 dataset using a heatmap (Shin et al., 2006). This comparison involves identical Mamba blocks—one trained without contrastive pre-training and the other with it. The resulting variations in distribution highlight the influence of our pre-training objectives, which enhance the model's ability to selectively focus on relevant features. The images illustrate the differences in the embedding space (Figure 7) and the refined distribution achieved through contrastive learning (Figure 6).

It is evident that the Mamba model without RCL struggles to effectively distinguish between irrelevant noise and valid time steps, and it fails to make effective selections within the time series. Additionally, the original Mamba model cannot adequately separate different time steps, maintaining high correlation, which indicates that new time step information fails to be effectively encoded and merely perturbs the coding. In contrast, Mamba with RCL effectively differentiates between valid time steps and filters out noise, mitigating the effects of long sequences and introducing more valid information, thereby improving the modeling of the entire sequence.

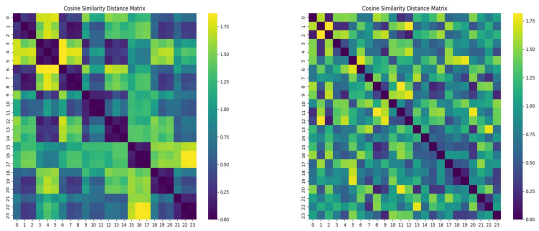

Figure 6: Embedding with contrastive pre-training result

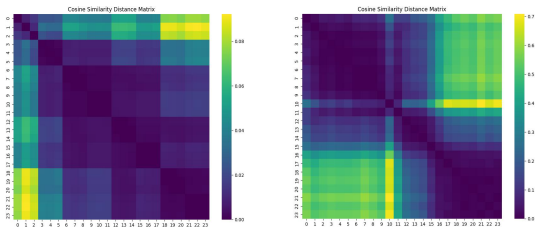

Figure 7: Embedding without pre-training result

6.2. *Visualization of clustering of Positive and Negative Cases*

We also visualized the detailed distribution of vectors using the UMAP technique for dimensionality reduction, where the original dimensionality of the embedding vectors is 32. UMAP is based on a theoretical framework rooted in Riemannian geometry and algebraic topology, resulting in a scalable and practical algorithm suitable for contrastive learning data (McInnes et al., 2020). In the visualizations (Figure 8), we randomly selected embedding vectors from input sequences and plotted the corresponding vectors for both positive and negative pairs in our method.

The clustering results demonstrate that the model can effectively distinguish between positive and negative examples, with positive examples clustering near the anchor and negative examples retreating farther away. The significance of this distinction is evident in the clustering results, indicating that our method can better recognize valid and invalid time steps, and possesses stronger differentiation and selection capabilities.

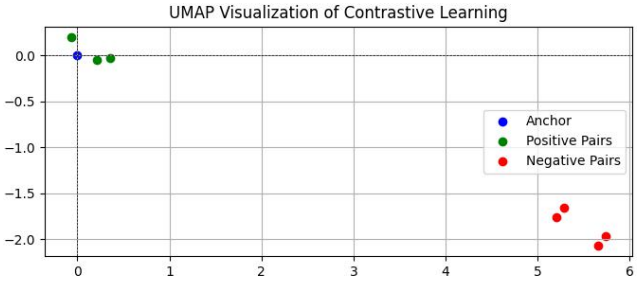

Figure 8: UMAP reduction results. Anchor points are randomly selected, and all other points are related to the anchor.

7. Related Work

7.1. *Models in Deep Time Series Forecasting*

Extensive research has been conducted to address time series forecasting problems, primarily focused on proposing new models that improve prediction accuracy. These models can be categorized into five primary groups: Transformer-based, RNN-basedHochreiter and Schmidhuber (1997), CNN-based, MLP-based, and Mamba-based. While emphasizing different aspects, these approaches aim to address key challenges of time series tasks.

Some MLP-based models, such as N-BeatsOreshkin et al. (2020) and N-HiTsChallu et al. (2022), utilize basis approximation and residual connections. TimesNet Wu et al. (2023), a CNN-based model, employs periodical segmentations in the frequency and time domains, extracting inter-period and intra-period patterns. TimeMixer Wang et al. (2024), built solely with MLP and pooling layers, excels by decomposing and mixing multi-scale data.

Transformer-based models like LogTransLi et al. (2020), InformerZhou et al. (2021), AutoformerWu et al. (2022), and FEDformerZhou et al. (2022) enhance adaptability using sparse attention and decomposition techniques. PatchTSTNie et al. (2023) segments time series into patches for denoising, while iTransformerLiu et al. (2024) redefines

time embeddings. Mamba-based models, like TimeMachineAhamed and Cheng (2024), unify channel-mixing and independence to refine content selection.

7.2. Contrastive Learning

Most contrastive self-supervised learning methods have been applied in vision Jaiswal et al. (2021) and multimodal learning Manzoor et al. (2024), leveraging high-level attributes that are easily distinguishable and less affected by noise. For example, images remain interpretable despite perturbations like color changes or geometric transformations, while multimodal methods enhance contrast by using cross-modality correlations, such as visual-textual pairing.

In contrast, applying contrastive learning to unimodal sequential data is less common and often requires tailored features. For instance, CodeRetriever Li et al. (2022) employs similarity contrastive loss to capture nuances in code sequences. Sequential recommendation Xie and Li (2024) and text summarization Xu et al. (2022) rely on specialized sequence representations and training techniques.

In time series, contrastive pre-training has improved representation learning. TS2Vec Yue et al. (2022) introduced a universal framework using context view augmentation and hierarchical contrastive learning. TF-C Zhang et al. (2022b) aligned time-based and frequency-based representations for better performance. InfoTS applied information theory to prioritize diverse and high-fidelity representations, while SoftCLT Lee et al. (2024) captured inter-sample and intra-temporal relationships through soft assignments.

These methods excel in representation learning for classification but are less effective for forecasting. Our approach pre-trains mamba models to capture recurrent noise patterns, enabling the direct application of pre-trained parameters to forecasting tasks, representing a novel and significant improvement over existing methods.

8. Conclusion

In this paper, we introduce Repetitive Contrastive Learning (RCL), a novel training paradigm designed to enhance the selective capabilities of Mamba blocks and enable the transfer of these parameters to various Mamba-based backbone models, improving their performance. RCL combines sequence repetition with intra-sequence and inter-sequence contrastive learning, strengthening Mamba blocks' ability to retain critical information and filter out noise. Through extensive experiments, we demonstrate RCL's effectiveness across multiple Mamba-based backbone models, significantly boosting their temporal prediction capabilities. From theoretical, qualitative, and quantitative perspectives, we validate the enhanced selective performance achieved by RCL and confirm that it adds no extra memory overhead. In future work, RCL could be adapted to other models with similar principles, such as RNNs and vanilla attention mechanisms.

Acknowledgments

This work is supported by the National Natural Science Foundation of China (Grant No. 62276008, 62250037, and 62076010), and partially supported by the National Key R&D of China (Grant #2022YFF0800601).

References

Ahamed, M.A., Cheng, Q., 2024. Timemachine: A time series is worth 4 mambas for long-term forecasting. URL: https://arxiv.org/abs/2403.09898, arXiv:2403.09898.

Challu, C., Olivares, K.G., Oreshkin, B.N., Garza, F., Mergenthaler-Canseco, M., Dubrawski, A., 2022. N-hits: Neural hierarchical interpolation for time series forecasting. URL: https://arxiv.org/abs/2201.12886, arXiv:2201.12886.

Cheng, X., Zhang, R., Zhou, J., Xu, W., 2023. Deeptransport: Learning spatial-temporal dependency for traffic condition forecasting. URL: https://arxiv.org/abs/1709.09585, arXiv:1709.09585.

Cruz-Camacho, E., Brown, K., Wang, X., Xu, X., Shu, K., Lan, Z., Ross, B., Carothers, C., 2024. Hybrid pdes simulation of hpc networks using zombie packets. ACM Trans. Model. Comput. Simul. URL: https://doi.org/10.1145/3682060, doi:10.1145/3682060. just Accepted.

Eldele, E., Ragab, M., Chen, Z., Wu, M., Kwoh, C.K., Li, X., Guan, C., 2023. Self-supervised contrastive representation learning for semi-supervised time-series classification. IEEE Transactions on Pattern Analysis and Machine Intelligence 45, 15604–15618. doi:10.1109/TPAMI.2023.3308189.

Gu, A., Dao, T., 2024. Mamba: Linear-time sequence modeling with selective state spaces. URL: https://arxiv.org/abs/2312.00752, arXiv:2312.00752.

Gu, A., Goel, K., Ré, C., 2022. Efficiently modeling long sequences with structured state spaces. URL: https://arxiv.org/abs/2111.00396, arXiv:2111.00396.

Haviv, D., Rivkind, A., Barak, O., 2019. Understanding and controlling memory in recurrent neural networks. URL: https://arxiv.org/abs/1902.07275, arXiv:1902.07275.
Hochreiter, S., Schmidhuber, J., 1997. Long short-term memory. Neural Comput. 9, 1735–1780. URL: https://doi.org/10.1162/neco.1997.9.8.1735, doi:10.1162/neco.1997.9.8.1735.
Huang, W., Pan, J., Tang, J., Ding, Y., Xing, Y., Wang, Y., Wang, Z., Hu, J., 2024. Ml-mamba: Efficient multi-modal large language model utilizing mamba-2. URL: https://arxiv.org/abs/2407.19832, arXiv:2407.19832.
Jaiswal, A., Babu, A.R., Zadeh, M.Z., Banerjee, D., Makedon, F., 2021. A survey on contrastive self-supervised learning. URL: https://arxiv.org/abs/2011.00362, arXiv:2011.00362.
Lee, S., Park, T., Lee, K., 2024. Soft contrastive learning for time series. URL: https://arxiv.org/abs/2312.16424, arXiv:2312.16424.
Li, S., Jin, X., Xuan, Y., Zhou, X., Chen, W., Wang, Y.X., Yan, X., 2020. Enhancing the locality and breaking the memory bottleneck of transformer on time series forecasting. URL: https://arxiv.org/abs/1907.00235, arXiv:1907.00235.
Li, S., Singh, H., Grover, A., 2024. Mamba-nd: Selective state space modeling for multi-dimensional data. URL: https://arxiv.org/abs/2402.05892, arXiv:2402.05892.
Li, T., Liu, Z., Shen, Y., Wang, X., Chen, H., Huang, S., 2023. Master: Market-guided stock transformer for stock price forecasting. URL: https://arxiv.org/abs/2312.15235, arXiv:2312.15235.
Li, X., Gong, Y., Shen, Y., Qiu, X., Zhang, H., Yao, B., Qi, W., Jiang, D., Chen, W., Duan, N., 2022. Coderetriever: Unimodal and bimodal contrastive learning for code search. URL: https://arxiv.org/abs/2201.10866, arXiv:2201.10866.
Liang, A., Jiang, X., Sun, Y., Shi, X., Li, K., 2024. Bi-mamba+: Bidirectional mamba for time series forecasting. URL: https://arxiv.org/abs/2404.15772, arXiv:2404.15772.
Liu, Y., Hu, T., Zhang, H., Wu, H., Wang, S., Ma, L., Long, M., 2024. itransformer: Inverted transformers are effective for time series forecasting. URL: https://arxiv.org/abs/2310.06625, arXiv:2310.06625.
Luo, D., Cheng, W., Wang, Y., Xu, D., Ni, J., Yu, W., Zhang, X., Liu, Y., Chen, Y., Chen, H., Zhang, X., 2023. Time series contrastive learning with information-aware augmentations. URL: https://arxiv.org/abs/2303.11911, arXiv:2303.11911.
Manzoor, M.A., Albarri, S., Xian, Z., Meng, Z., Nakov, P., Liang, S., 2024. Multimodality representation learning: A survey on evolution, pretraining and its applications. URL: https://arxiv.org/abs/2302.00389, arXiv:2302.00389.
McInnes, L., Healy, J., Melville, J., 2020. Umap: Uniform manifold approximation and projection for dimension reduction. URL: https://arxiv.org/abs/1802.03426, arXiv:1802.03426.
Ming, Y., Cao, S., Zhang, R., Li, Z., Chen, Y., Song, Y., Qu, H., 2017. Understanding hidden memories of recurrent neural networks, in: 2017 IEEE Conference on Visual Analytics Science and Technology (VAST), pp. 13–24. doi:10.1109/VAST.2017.8585721.
Nam, H., Kim, J., Yeom, J., 2024. An adversarial learning approach to irregular time-series forecasting. URL: https://arxiv.org/abs/2411.19341, arXiv:2411.19341.
Nie, Y., Nguyen, N.H., Sinthong, P., Kalagnanam, J., 2023. A time series is worth 64 words: Long-term forecasting with transformers. URL: https://arxiv.org/abs/2211.14730, arXiv:2211.14730.
van den Oord, A., Li, Y., Vinyals, O., 2019. Representation learning with contrastive predictive coding. URL: https://arxiv.org/abs/1807.03748, arXiv:1807.03748.
Oord, A.v.d., Li, Y., Vinyals, O., 2018. Representation learning with contrastive predictive coding. arXiv preprint arXiv:1807.03748 .
Oreshkin, B.N., Carpov, D., Chapados, N., Bengio, Y., 2020. N-beats: Neural basis expansion analysis for interpretable time series forecasting. URL: https://arxiv.org/abs/1905.10437, arXiv:1905.10437.
Patro, B.N., Agneeswaran, V.S., 2024. Simba: Simplified mamba-based architecture for vision and multivariate time series. URL: https://arxiv.org/abs/2403.15360, arXiv:2403.15360.
Rahutomo, F., Kitasuka, T., Aritsugi, M., 2012. Semantic cosine similarity.
Ramponi, G., Protopapas, P., Brambilla, M., Janssen, R., 2019. T-cgan: Conditional generative adversarial network for data augmentation in noisy time series with irregular sampling. URL: https://arxiv.org/abs/1811.08295, arXiv:1811.08295.
Shin, J.H., Blay, S., McNeney, B., Graham, J., 2006. Ldheatmap: An r function for graphical display of pairwise linkage disequilibria between single nucleotide polymorphisms. Journal of Statistical Software, Code Snippets 16, 1–9. URL: https://www.jstatsoft.org/index.php/jss/article/view/v016c03, doi:10.18637/jss.v016.c03.
Sun, Y., Zhang, F., 2023. Quarterly electricity consumption prediction based on time series decomposition method and gray model. Environmental Science and Pollution Research 30, 95410–95424. URL: https://doi.org/10.1007/s11356-023-29044-0, doi:10.1007/s11356-023-29044-0.
Vaswani, A., Shazeer, N., Parmar, N., Uszkoreit, J., Jones, L., Gomez, A.N., Kaiser, L., Polosukhin, I., 2023. Attention is all you need. URL: https://arxiv.org/abs/1706.03762, arXiv:1706.03762.
Wang, S., Wu, H., Shi, X., Hu, T., Luo, H., Ma, L., Zhang, J.Y., Zhou, J., 2024. Timemixer: Decomposable multiscale mixing for time series forecasting. URL: https://arxiv.org/abs/2405.14616, arXiv:2405.14616.
Wang, W., Yao, L., Chen, L., Lin, B., Cai, D., He, X., Liu, W., 2021. Crossformer: A versatile vision transformer hinging on cross-scale attention. URL: https://arxiv.org/abs/2108.00154, arXiv:2108.00154.
Wen, Q., Zhou, T., Zhang, C., Chen, W., Ma, Z., Yan, J., Sun, L., 2023. Transformers in time series: A survey. URL: https://arxiv.org/abs/2202.07125, arXiv:2202.07125.
Wu, H., Hu, T., Liu, Y., Zhou, H., Wang, J., Long, M., 2023. Timesnet: Temporal 2d-variation modeling for general time series analysis. URL: https://arxiv.org/abs/2210.02186, arXiv:2210.02186.
Wu, H., Xu, J., Wang, J., Long, M., 2022. Autoformer: Decomposition transformers with auto-correlation for long-term series forecasting. URL: https://arxiv.org/abs/2106.13008, arXiv:2106.13008.
Wu, M., Zhuang, C., Mosse, M., Yamins, D., Goodman, N., 2020. On mutual information in contrastive learning for visual representations. URL: https://arxiv.org/abs/2005.13149, arXiv:2005.13149.
Xie, Z., Li, J., 2024. Simple debiased contrastive learning for sequential recommendation. Knowledge-Based Systems 300, 112257. URL: https://www.sciencedirect.com/science/article/pii/S0950705124008918, doi:https://doi.org/10.1016/j.knosys.2024.112257.

Xu, S., Zhang, X., Wu, Y., Wei, F., 2022. Sequence level contrastive learning for text summarization. URL: https://arxiv.org/abs/2109.03481, arXiv:2109.03481.

Yue, Z., Wang, Y., Duan, J., Yang, T., Huang, C., Tong, Y., Xu, B., 2022. Ts2vec: Towards universal representation of time series. URL: https://arxiv.org/abs/2106.10466, arXiv:2106.10466.

Zeng, A., Chen, M., Zhang, L., Xu, Q., 2022. Are transformers effective for time series forecasting? URL: https://arxiv.org/abs/2205.13504, arXiv:2205.13504.

Zhang, C., Li, Q., Hua, L., Song, D., 2020. Assessing the memory ability of recurrent neural networks. URL: https://arxiv.org/abs/2002.07422, arXiv:2002.07422.

Zhang, G., Yang, D., Galanis, G., Androulakis, E., 2022a. Solar forecasting with hourly updated numerical weather prediction. Renewable and Sustainable Energy Reviews 154, 111768. URL: https://www.sciencedirect.com/science/article/pii/S1364032121010364, doi:https://doi.org/10.1016/j.rser.2021.111768.

Zhang, W., Huang, J., Wang, R., Wei, C., Huang, W., Qiao, Y., 2024. Integration of mamba and transformer – mat for long-short range time series forecasting with application to weather dynamics. URL: https://arxiv.org/abs/2409.08530, arXiv:2409.08530.

Zhang, X., Zhao, Z., Tsiligkaridis, T., Zitnik, M., 2022b. Self-supervised contrastive pre-training for time series via time-frequency consistency. URL: https://arxiv.org/abs/2206.08496, arXiv:2206.08496.

Zhou, H., Zhang, S., Peng, J., Zhang, S., Li, J., Xiong, H., Zhang, W., 2021. Informer: Beyond efficient transformer for long sequence time-series forecasting. URL: https://arxiv.org/abs/2012.07436, arXiv:2012.07436.

Zhou, T., Ma, Z., Wen, Q., Wang, X., Sun, L., Jin, R., 2022. Fedformer: Frequency enhanced decomposed transformer for long-term series forecasting. URL: https://arxiv.org/abs/2201.12740, arXiv:2201.12740.

Zhu, Y., Jiang, B., Jin, H., Zhang, M., Gao, F., Huang, J., Lin, T., Wang, X., 2023. Networked time series prediction with incomplete data via generative adversarial network. URL: https://arxiv.org/abs/2110.02271, arXiv:2110.02271.

Appendix A. Reproducibility Statement

We provide simplified code available at this Anonymous Github link[1]. You can use this code to reproduce our results by referring to the parameters outlined in the paper.

Appendix B. Additional Experimental Results

Appendix B.1. Comprehensive Results of Comparison with Temporal Model

Table B.10 provides the detailed comparative results across the four prediction horizons, where we achieve significant improvements and attain state-of-the-art performance across multiple prediction lengths.

Model		**TimeMachine***		TimeMachine		**Bi-Mamba***		Bi-Mamba		iTransformer		TimeMixer		CrossFormer		PatchTST		TimesNet		FEDFormer		Informer		N-HiTS		N-BEATS	
Metric		MAE	MSE	MAE	MSE	MAE	MSE	MAE	MSE	MAE	MSE	MAE	MSE	MAE	MSE	MAE	MSE	MAE	MSE	MAE	MSE	MAE	MSE	MAE	MSE	MAE	MSE
ETTh1	96	**0.387**	0.379	0.391	0.383	0.389	0.379	0.395	0.381	0.405	0.386	0.400	**0.375**	0.448	0.423	0.419	0.414	0.402	0.384	0.419	0.376	0.713	0.865	0.397	0.394	0.415	0.406
	192	**0.420**	0.440	0.423	0.440	0.421	**0.425**	0.428	0.427	0.436	0.441	0.421	0.429	0.474	0.471	0.445	0.460	0.429	0.436	0.448	0.420	0.792	1.008	0.434	0.478	0.514	0.535
	336	**0.442**	0.482	0.446	0.490	0.456	**0.481**	0.459	0.484	0.458	0.487	0.458	0.484	0.546	0.570	0.466	0.501	0.469	0.491	0.465	0.459	0.809	1.107	0.489	0.508	0.499	0.495
	720	**0.466**	**0.488**	0.470	0.496	0.496	0.496	0.496	0.516	0.491	0.503	0.482	0.498	0.621	0.653	0.488	0.500	0.500	0.521	0.507	0.506	0.865	1.181	0.499	0.519	0.523	0.523
ETTh2	96	**0.330**	**0.282**	0.334	0.291	0.347	0.300	0.349	0.307	0.349	0.297	0.341	0.289	0.584	0.745	0.348	0.302	0.374	0.340	0.397	0.358	1.525	3.755	0.346	0.303	0.331	0.233
	192	**0.382**	**0.355**	0.385	0.369	0.394	0.373	0.398	0.377	0.400	0.380	0.392	0.372	0.656	0.877	0.400	0.388	0.414	0.402	0.439	0.429	1.931	5.602	0.417	0.396	0.432	0.372
	336	0.420	0.412	0.428	0.421	0.429	0.434	0.434	0.435	0.432	0.428	**0.414**	**0.386**	0.731	1.043	0.433	0.426	0.452	0.452	0.487	0.496	1.835	4.721	0.514	0.468	0.507	0.479
	720	**0.430**	**0.412**	0.439	0.424	0.602	0.731	0.597	0.715	0.445	0.427	0.434	0.412	0.763	1.104	0.446	0.431	0.468	0.462	0.474	0.463	1.625	3.647	0.514	0.518	0.616	0.560
ETTm1	96	**0.346**	**0.318**	0.361	0.334	0.358	0.332	0.364	0.332	0.368	0.334	0.357	0.320	0.426	0.404	0.367	0.329	0.375	0.338	0.419	0.379	0.571	0.672	0.371	0.352	0.378	0.364
	192	**0.377**	0.375	0.379	0.379	0.384	0.369	0.389	0.378	0.391	0.377	0.381	**0.361**	0.451	0.450	0.385	0.367	0.387	0.374	0.441	0.426	0.669	0.795	0.396	0.389	0.385	0.381
	336	**0.387**	0.396	0.394	0.401	0.407	0.404	0.412	0.405	0.420	0.426	0.404	**0.390**	0.515	0.532	0.410	0.399	0.411	0.410	0.459	0.445	0.871	1.212	0.393	0.413	0.401	0.399
	720	**0.429**	0.455	0.431	0.467	0.441	0.458	0.452	0.466	0.459	0.491	0.441	**0.454**	0.589	0.666	0.439	0.454	0.450	0.478	0.490	0.543	0.823	1.166	0.502	0.487	0.441	0.529
ETTm2	96	**0.251**	**0.173**	0.253	0.175	0.271	0.186	0.270	0.188	0.264	0.180	0.258	0.175	0.366	0.287	0.259	0.175	0.267	0.187	0.287	0.203	0.453	0.365	0.255	0.176	0.263	0.184
	192	**0.293**	0.238	0.294	0.238	0.313	0.254	0.315	0.257	0.309	0.250	0.299	**0.237**	0.492	0.414	0.302	0.241	0.309	0.249	0.328	0.269	0.563	0.533	0.305	0.245	0.337	0.273
	336	**0.333**	0.299	0.337	0.307	0.364	0.316	0.387	0.392	0.348	0.311	0.340	**0.298**	0.542	0.597	0.343	0.305	0.351	0.321	0.366	0.325	0.887	1.363	0.346	0.295	0.355	0.309
	720	**0.392**	0.402	0.394	0.407	0.413	0.404	0.430	0.429	0.407	0.412	0.396	**0.391**	1.042	1.730	0.400	0.402	0.403	0.408	0.415	0.421	1.338	3.379	0.413	0.401	0.425	0.411
Traffic	96	0.299	0.484	0.306	0.498	0.276	0.579	0.279	0.587	**0.268**	**0.395**	0.285	0.462	0.290	0.522	0.359	0.544	0.321	0.593	0.366	0.587	0.368	0.274	0.282	0.402	0.282	0.398
	192	**0.273**	**0.412**	0.274	0.417	0.308	0.625	0.306	0.630	0.276	0.417	0.296	0.473	0.293	0.530	0.354	0.540	0.336	0.617	0.373	0.604	0.386	0.296	0.297	0.42	0.293	0.409
	336	**0.279**	**0.429**	0.281	0.433	0.311	0.666	0.307	0.659	0.283	0.433	0.296	0.498	0.305	0.558	0.358	0.551	0.336	0.629	0.383	0.621	0.394	0.300	0.313	0.448	0.318	0.449
	720	**0.298**	**0.459**	0.300	0.467	0.336	0.689	0.338	0.702	0.302	0.467	0.313	0.506	0.328	0.589	0.375	0.586	0.350	0.640	0.382	0.626	0.439	0.373	0.353	0.539	0.391	0.589
Electricity	96	0.259	0.183	0.261	0.187	0.261	0.182	0.263	0.185	**0.240**	**0.148**	0.247	0.153	0.314	0.219	0.285	0.195	0.272	0.168	0.308	0.193	0.391	0.719	0.285	0.182	0.235	0.173
	192	**0.246**	**0.152**	0.250	0.158	0.270	0.188	0.272	0.191	0.253	0.162	0.256	0.166	0.322	0.231	0.289	0.199	0.289	0.184	0.315	0.201	0.379	0.696	0.300	0.228	0.287	0.185
	336	**0.261**	**0.169**	0.268	0.172	0.283	0.200	0.290	0.212	0.269	0.178	0.277	0.185	0.337	0.246	0.305	0.215	0.300	0.198	0.329	0.214	0.420	0.777	0.354	0.242	0.355	0.257
	720	**0.295**	**0.201**	0.298	0.207	0.317	0.255	0.323	0.259	0.317	0.225	0.310	0.225	0.363	0.280	0.337	0.256	0.320	0.220	0.355	0.246	0.472	0.864	0.377	0.331	0.438	0.369

Table B.10: Comparison results with temporal model. Bolded numbers indicate optimal results and underscores indicate sub-optimal results.

Appendix B.2. Detail Comparison of Improvements

To demonstrate that pre-training Mamba blocks with RCL can effectively enhance the temporal prediction capabilities of Mamba-based models, we present the performance improvements of four Mamba-based models after using pre-trained parameters. We conducted extensive testing on six datasets, each with an input length of 96 and prediction lengths of $\{96, 192, 336, 720\}$. To clearly illustrate the performance improvements, we provide the percentage increase in MSE and MAE when using pre-trained parameters compared to not using them, as shown by the up-rate in Table B.12.

The results indicate that, for the vast majority of datasets and prediction lengths, the parameters obtained through our method enhance the predictive performance of Mamba-based models, demonstrating that our approach is generally effective. By pre-training a Mamba block and using the pre-trained parameters to initialize all mamba blocks in Mamba-based model, the original model's temporal prediction performance can be significantly improved.

Appendix B.3. Standard Deviation

We provided the standard deviation of experimental results across multiple datasets. As Shown in Table B.11.It can be observed that using RCL parameters for initialization results in a standard deviation similar to not using them, indicating that our method enhances performance without introducing additional instability.

[1] https://anonymous.4open.science/r/PretrainMamba-DD5B/

Model		**TimeMachine***		TimeMachine		**Bi-Mamba***		Bi-Mamba	
Metric		MAE	MSE	MAE	MSE	MAE	MSE	MAE	MSE
ETTh1	96	±0.001	±0.002	±0.002	±0.002	±0.003	±0.007	±0.005	±0.007
	192	±0.002	±0.005	±0.004	±0.008	±0.003	±0.006	±0.006	±0.007
	336	±0.002	±0.006	±0.003	±0.005	±0.006	±0.005	±0.009	±0.013
	720	±0.006	±0.006	±0.009	±0.013	±0.007	±0.009	±0.008	±0.015
ETTh2	96	±0.001	±0.001	±0.005	±0.007	±0.001	±0.002	±0.001	±0.001
	192	±0.002	±0.001	±0.006	±0.006	±0.002	±0.002	±0.001	±0.002
	336	±0.004	±0.006	±0.009	±0.013	±0.003	±0.003	±0.003	±0.004
	720	±0.006	±0.006	±0.010	±0.009	±0.006	±0.006	±0.007	±0.010
ETTm1	96	±0.002	±0.002	±0.002	±0.001	±0.002	±0.002	±0.003	±0.002
	192	±0.003	±0.006	±0.003	±0.003	±0.002	±0.004	±0.003	±0.004
	336	±0.003	±0.005	±0.004	±0.004	±0.003	±0.005	±0.004	±0.005
	720	±0.006	±0.009	±0.005	±0.007	±0.004	±0.004	±0.003	±0.004
ETTm2	96	±0.001	±0.001	±0.001	±0.001	±0.001	±0.001	±0.001	±0.001
	192	±0.001	±0.002	±0.001	±0.001	±0.001	±0.001	±0.001	±0.001
	336	±0.003	±0.005	±0.002	±0.006	±0.002	±0.003	±0.002	±0.002
	720	±0.005	±0.005	±0.004	±0.006	±0.004	±0.005	±0.003	±0.004
Traffic	96	±0.005	±0.004	±0.004	±0.003	±0.002	±0.002	±0.003	±0.005
	192	±0.006	±0.005	±0.003	±0.003	±0.001	±0.002	±0.001	±0.002
	336	±0.006	±0.006	±0.005	±0.005	±0.002	±0.002	±0.001	±0.003
	720	±0.005	±0.007	±0.006	±0.009	±0.003	±0.003	±0.001	±0.002
Electricity	96	±0.001	±0.002	±0.001	±0.002	±0.001	±0.001	±0.001	±0.001
	192	±0.001	±0.001	±0.002	±0.002	±0.001	±0.001	±0.002	±0.002
	336	±0.002	±0.002	±0.001	±0.001	±0.001	±0.002	±0.001	±0.003
	720	±0.001	±0.002	±0.001	±0.001	±0.001	±0.002	±0.002	±0.002

Table B.11: Standard deviation of experimental results

			ETTh1		ETTh2		ETTm1		ETTm2		Traffic		Electricity	
			MAE	MSE	MAE	MSE	MAE	MSE	MAE	MSE	MAE	MSE	MAE	MSE
Mamba	96	w/o	0.6546	0.7672	1.4013	2.8442	0.5053	0.5432	0.5763	0.6008	0.4939	1.0279	0.4232	0.3926
		w	0.5974	0.6542	1.1536	2.0506	0.4798	0.4946	0.5646	0.5677	0.4604	0.9076	0.4168	0.3879
		up-rate%	**8.7382**	**14.729**	**17.676**	**27.902**	**5.0465**	**8.9470**	**2.0302**	**5.5093**	**6.7827**	**11.704**	**1.5123**	**1.1.971**
	192	w/o	0.6298	0.7115	1.2371	2.1642	0.5126	0.5866	0.6670	0.8471	0.5617	1.1962	0.4298	0.4053
		w	0.6021	0.7127	1.0509	1.9490	0.4970	0.5524	0.5655	0.5573	0.5610	1.1877	0.4288	0.4130
		up-rate%	4.3982	-0.1687	**15.0513**	**9.9436**	**3.0433**	**5.8302**	**15.2174**	**34.2108**	**0.1246**	**0.7106**	0.2327	-1.8998
	336	w/o	0.6383	0.7210	1.2341	2.1528	0.8172	1.4569	0.7052	0.9220	0.6025	1.3079	0.4354	0.4108
		w	0.6084	0.7145	1.0497	1.9485	0.8008	1.4479	0.6270	0.6842	0.5848	1.2560	0.4324	0.4176
		up-rate%	**4.6843**	**0.9015**	**14.9421**	**9.4900**	**2.0069**	**0.6178**	**11.0891**	**25.7918**	**2.9378**	**3.9682**	0.6890	-1.6553
	720	w/o	0.6776	0.7727	1.2206	2.1005	0.8235	1.4557	0.7374	0.9942	0.4893	1.0108	0.4529	0.4326
		w	0.6461	0.7556	1.0541	1.9537	0.8142	1.4588	0.6682	0.7811	0.4645	0.9189	0.4447	0.4320
		up-rate%	**4.6488**	**2.2130**	**13.6408**	**6.9888**	1.1293	-0.2130	**9.3843**	**21.4343**	**5.0685**	**9.0918**	**1.8106**	**0.1387**
iMamba	96	w/o	0.4987	0.4928	0.6926	0.9084	0.4316	0.3998	0.4160	0.3666	0.3234	0.6538	0.2627	0.1857
		w	0.4472	0.4278	0.6833	0.8595	0.3970	0.3669	0.3304	0.2469	0.2913	0.6003	0.2597	0.1827
		up-rate%	**10.3268**	**13.1899**	**1.3428**	**5.3831**	**8.0167**	**8.2291**	**20.5769**	**32.6514**	**9.9258**	**8.1829**	**1.1420**	**1.6155**
	192	w/o	0.5075	0.5320	1.0228	1.8207	0.4500	0.4390	0.4973	0.4949	0.3129	0.6354	0.2801	0.2047
		w	0.4871	0.5143	0.9430	1.5825	0.4356	0.4174	0.4763	0.4557	0.3091	0.6335	0.2788	0.2025
		up-rate%	**4.0197**	**3.3271**	**7.8021**	**13.0829**	**3.2000**	**4.9203**	**4.2228**	**7.9208**	**1.2144**	**0.2990**	**0.4641**	**1.0747**
	336	w/o	0.5125	0.5498	1.0727	2.0417	0.4909	0.5085	0.7932	1.0322	0.3233	0.6605	0.2987	0.2238
		w	0.4750	0.4992	0.9913	1.7052	0.4677	0.4998	0.5854	0.6272	0.3216	0.6645	0.2975	0.2222
		up-rate%	**7.3171**	**9.2033**	**7.5883**	**16.4814**	**4.7260**	**1.7109**	**26.1977**	**39.2366**	0.5258	-0.6056	**0.4017**	**0.7149**
	720	w/o	0.5418	0.5818	1.0534	1.8199	0.6238	0.7306	1.0698	2.0298	0.3486	0.7105	0.3342	0.2683
		w	0.5391	0.5640	1.0172	1.7220	0.5120	0.5534	0.9936	1.5644	0.3475	0.7172	0.3323	0.2627
		up-rate%	**0.4983**	**3.0595**	**3.4365**	**5.3794**	**17.9224**	**24.2540**	**7.1228**	**22.9284**	0.3155	-0.9430	**0.5685**	**2.0872**
TimeMachine	96	w/o	0.3905	0.3833	0.3344	0.2911	0.3606	0.3342	0.2525	0.1746	0.3064	0.4983	0.2611	0.1872
		w	0.3869	0.3787	0.3298	0.2822	0.3458	0.3179	0.2508	0.1731	0.2991	0.4844	0.2586	0.1826
		up-rate%	**0.9219**	**1.2001**	**1.3756**	**3.0574**	**4.1043**	**4.8773**	**0.6733**	**0.8591**	**2.3825**	**2.7895**	**0.9575**	**2.4573**
	192	w/o	0.4225	0.4401	0.3851	0.3685	0.3785	0.3787	0.2941	0.2381	0.2740	0.4170	0.2500	0.1580
		w	0.4202	0.4399	0.3821	0.3551	0.3770	0.3750	0.2930	0.2381	0.2732	0.4115	0.2460	0.1520
		up-rate%	**0.5444**	**0.0454**	**0.7790**	**3.6364**	**0.3963**	**0.9770**	**0.3740**	**0.0000**	**0.2920**	**1.3189**	**1.6000**	**3.7975**
	336	w/o	0.4458	0.4902	0.4281	0.4206	0.3937	0.4010	0.3371	0.3066	0.2810	0.4330	0.2680	0.1720
		w	0.4419	0.4824	0.4201	0.4119	0.3867	0.3956	0.3327	0.2991	0.2790	0.4290	0.2610	0.1690
		up-rate%	**0.8748**	**1.5912**	**1.8687**	**2.0685**	**1.7780**	**1.3466**	**1.3053**	**2.4462**	**0.7117**	**0.9238**	**2.6119**	**1.7442**
	720	w/o	0.4702	0.4959	0.4386	0.4243	0.4310	0.4670	0.3940	0.4073	0.3000	0.4670	0.2980	0.2070
		w	0.4656	0.4883	0.4295	0.4119	0.4291	0.4552	0.3920	0.4018	0.2980	0.4590	0.2950	0.2010
		up-rate%	**0.9783**	**1.5326**	**2.0748**	**2.9225**	**0.4408**	**2.5268**	**0.5076**	**1.3504**	**0.6667**	**1.7131**	**1.0067**	**2.8986**
Bi-Mamba	96	w/o	0.3948	0.3813	0.3443	0.2937	0.3641	0.3319	0.2704	0.1883	0.2786	0.587	0.2629	0.185
		w	0.3893	0.3794	0.3462	0.2955	0.3578	0.3316	0.2707	0.1857	0.2761	0.5787	0.2611	0.1818
		up-rate%	**1.3931**	**0.4983**	**1.7303**	**0.0904**	**0.9829**	**1.2814**	-0.1109	**1.3808**	**0.8973**	**1.4140**	**0.6847**	**1.7280**
	192	w/o	0.4280	0.4270	0.3977	0.3772	0.3894	0.3780	0.3145	0.2572	0.3057	0.6301	0.2715	0.1914
		w	0.4210	0.4250	0.3935	0.3733	0.3840	0.3692	0.3131	0.2544	0.3081	0.6250	0.2698	0.1881
		up-rate%	**1.6355**	**0.4684**	**1.0561**	**1.0339**	**1.3867**	**2.3280**	**0.4452**	**1.0886**	-0.7851	0.8094	**0.6262**	**1.7241**
	336	w/o	0.4593	0.4838	0.4340	0.4354	0.4119	0.4045	0.3871	0.3915	0.3068	0.6585	0.2896	0.2117
		w	0.4563	0.4805	0.4286	0.4344	0.4069	0.4036	0.3644	0.3158	0.3107	0.6659	0.2831	0.1999
		up-rate%	**0.6532**	**0.6821**	**1.2442**	**0.2297**	**1.2139**	**0.2225**	**5.8641**	**19.3359**	-1.2712	-1.1238	**2.2445**	**5.5739**
	720	w/o	0.4963	0.5164	0.5970	0.7150	0.4517	0.4659	0.4300	0.4292	0.3384	0.7015	0.3228	0.2591
		w	0.4960	0.4962	0.6020	0.7310	0.4413	0.4579	0.4131	0.4044	0.3364	0.6894	0.3174	0.2547
		up-rate%	**0.0604**	**3.9117**	-0.8375	-2.2378	**2.3024**	**1.7171**	**3.9302**	**5.7782**	**0.5910**	**1.7249**	**1.6729**	**1.6982**

Table B.12: Detail Comparison of performance improvement by replacing parameters obtained by RCL. w/o denotes no parameter replacement, w denotes parameter replacement, and up-rate represents the improvement rate.